

REPORT DOCUMENTATION PAGE				Form Approved OMB No. 0704-0188	
Public reporting burden for this collection of information is estimated to average 1 hour per response, including the time for reviewing instructions, searching existing data sources, gathering and maintaining the data needed, and completing and reviewing this collection of information. Send comments regarding this burden estimate or any other aspect of this collection of information, including suggestions for reducing this burden to Department of Defense, Washington Headquarters Services, Directorate for Information Operations and Reports (0704-0188), 1215 Jefferson Davis Highway, Suite 1204, Arlington, VA 22202-4302. Respondents should be aware that notwithstanding any other provision of law, no person shall be subject to any penalty for failing to comply with a collection of information if it does not display a currently valid OMB control number. PLEASE DO NOT RETURN YOUR FORM TO THE ABOVE ADDRESS.					
1. REPORT DATE (DD-MM-YYYY) 01-08-2006		2. REPORT TYPE Final Performance Report		3. DATES COVERED (From - To) 1 May 2005 to 30 April 2006	
4. TITLE AND SUBTITLE High-Pressure Liquid Chromatograph with Mass Spectrometric Detection for Analysis of Supercritical Fuels Pyrolysis Products				5a. CONTRACT NUMBER	
				5b. GRANT NUMBER FA9550-05-1-0253	
				5c. PROGRAM ELEMENT NUMBER 61103F	
6. AUTHOR(S) Mary J. Wornat, Michelle L. Somers, Jennifer W. McClaine, and Jorge O. Ona				5d. PROJECT NUMBER 5094	
				5e. TASK NUMBER US	
				5f. WORK UNIT NUMBER FA9550-05-1-0253	
7. PERFORMING ORGANIZATION NAME(S) AND ADDRESS(ES) Louisiana State University Department of Chemical Engineering South Stadium Drive Baton Rouge, LA 70803				8. PERFORMING ORGANIZATION REPORT NUMBER	
9. SPONSORING / MONITORING AGENCY NAME(S) AND ADDRESS(ES) AFOSR/NA 875 North Randolph Street Suite 325, Room 3112 Arlington, VA 22203-1768				10. SPONSOR/MONITOR'S ACRONYM(S)	
				11. SPONSOR/MONITOR'S REPORT NUMBER(S)	
12. DISTRIBUTION / AVAILABILITY STATEMENT Approved for public release; distribution unlimited					
13. SUPPLEMENTARY NOTES					
14. ABSTRACT A high-pressure liquid chromatograph with ultraviolet-visible diode-array detection and mass spectrometer (HPLC/UV/MS), purchased with DURIP funds, was used to analyze polycyclic aromatic hydrocarbons (PAH) produced in supercritical pyrolysis experiments with the model fuels 1-methylnaphthalene and toluene. The HPLC/UV/MS instrument facilitated the identification of fifteen 5- to 9-ring PAH from supercritical 1-methylnaphthalene pyrolysis and five 7- to 9-ring PAH from supercritical toluene pyrolysis—none of which had ever before been identified as products of these fuels. Most of the newly identified products were large PAH thought to be intermediates in the formation of carbonaceous solids. The new PAH product identifications, along with determination of which PAH were not formed, contributed to the elucidation of radical reaction pathways responsible for PAH formation from aromatic fuels in the supercritical pyrolysis environment. Use of the HPLC/UV/MS instrument in the analysis of a stressed Fischer-Tropsch synthetic jet fuel sample from United Technologies Research Center led to the identification of fifteen 6- to 10-ring PAH, not previously identified by HPLC/UV alone—four of which had never before been unequivocally identified in the products of any fuel in any context.					
15. SUBJECT TERMS high-pressure liquid chromatography, ultraviolet-visible absorption spectroscopy, mass spectrometry, polycyclic aromatic hydrocarbons, carbonaceous solid deposits, hypersonic aircraft, supercritical fuel pyrolysis, PAH formation chemistry					
16. SECURITY CLASSIFICATION OF:			17. LIMITATION OF ABSTRACT	18. NUMBER OF PAGES	19a. NAME OF RESPONSIBLE PERSON
a. REPORT Unclassified	b. ABSTRACT Unclassified	c. THIS PAGE Unclassified			Dr. Julian Tishkoff
			UL	52	19b. TELEPHONE NUMBER (include area code) (703) 696-8478

**High-Pressure Liquid Chromatograph with Mass Spectrometric Detection
for Analysis of Supercritical Fuels Pyrolysis Products**

Table of Contents

Cover Page	i
Table of Contents	ii
Introduction	1
Experimental Equipment and Procedures	3
Reactor System	3
Product Analysis	4
Illustration of How the HPLC/UV/MS Technique Works	7
Results and Discussion	8
Model Experiments with 1-Methylnaphthalene	8
Model Experiments with Toluene	20
Analysis of Stressed Fischer-Tropsch Synthetic Jet Fuel S-8 from UTRC	23
Summary	25
Publications and Presentations	27
References	28
Tables	32
Figures	

Introduction

The fuels used in the next generation of hypersonic aircraft will have to operate under very high pressures and will have to sustain very high heat loads (*e.g.*, $\geq 30,000$ BTU/min) in order to meet aircraft cooling requirements [1-3]. Predictions indicate that within the fuel lines and injection system, where residence times can be several minutes, fuel temperatures and pressures may reach or exceed 540 °C and 150 atm [2]. In a recent review article, Edwards [4] states that “a Mach 8 scramjet engine could require fuel heat-sink levels of 3500 kJ/kg, equivalent to temperatures on the order of 700 °C.” These ranges of temperature and pressure substantially exceed the critical temperatures and pressures of most pure hydrocarbons and jet fuels such as JP-7 and JP-8 [1,4], so hydrocarbon fuels under these conditions will necessarily be supercritical fluids. These temperatures and pressures will also cause the fuel to undergo pyrolytic reactions, which have the potential of forming carbonaceous solids that can clog fuel lines, foul fuel nozzles, and lead to undesirable or even disastrous effects for the aircraft. In the context of hypersonic applications, carbonaceous solids formation has been identified as “the principal engine operability issue that will affect hydrocarbon fuel cooling technology” [5].

In order to develop reliable fuel systems for high-speed aircraft that will not be subject to solid deposit formation, we need a thorough understanding of the pyrolysis behavior of candidate fuels under the supercritical conditions that they will be operating. Of particular interest are the reactions leading to polycyclic aromatic hydrocarbons (PAH), which serve as precursors to the carbonaceous solids. To better understand the reaction mechanisms and kinetics of fuel pyrolysis and PAH formation under supercritical conditions, we are currently engaged in AFOSR-sponsored research (Grant Number FA9550-04-1-0005) on the supercritical pyrolysis of model fuels representing jet fuel components. One of the primary objectives of our research is to better elucidate the large-PAH-to-solids transformation, by examining detailed PAH compositional changes within the regime of near-incipient solids formation.

In order to resolve these important compositional changes, for some years we have successfully employed [6,7] high-pressure liquid chromatography (HPLC) with diode-array

ultraviolet-visible (UV) absorbance detection, a technique that leads to the isomer-specific identification of product PAH by matching their “fingerprint” UV absorbance spectra with those of PAH reference standards. For the large PAH of particular interest as carbonaceous solids precursors, however, HPLC/UV analysis alone has its limitations, since for large PAH, there are hundreds and even thousands of possible structures, and the number for which there are reference standards is very small.

Acquisition, through DURIP funds, of a new high-pressure liquid chromatograph with UV diode-array detector and mass spectrometer—HPLC/UV/MS—has greatly enhanced our ability to analyze large PAH, however, in addition to other PAH rarely encountered in combustion contexts but specific to the supercritical fuel pyrolysis environment. By establishing the molecular C_xH_y formula of an unknown PAH product component, the mass spectrum from the HPLC/UV/MS instrument serves to narrow the field of possible candidates to a particular PAH isomer group, facilitating the ultimate designation of the exact molecular structure by the fingerprint UV spectrum.

The present report illustrates how the new HPLC/UV/MS instrument (Agilent Technologies Model 1100, purchased for \$165,790 on Grant Number FA9550-05-1-0253) has greatly aided our AFOSR-sponsored research on supercritical fuels pyrolysis by enabling us to determine the identities of many of the PAH products of our experiments with model fuels. The instrument also enables us to determine which PAH are not produced in a given reaction environment. Knowing which PAH are produced and which are not has contributed significantly to our ability to discern reaction mechanisms. In addition to the model fuel studies, at the suggestion of Dr. Tim Edwards at AFRL, we have used the new HPLC/UV/MS instrument to analyze PAH produced by fuels particularly prone to forming solids, which have been exposed to scramjet-like supercritical conditions in tests performed at United Technologies Research Center (UTRC). These samples have been provided to us by Dr. He Huang at UTRC.

In the following, we describe the supercritical fuels pyrolysis reactor used in the model fuel experiments that generate most of the samples we analyze on the new HPLC/UV/MS. We then

describe our product analysis procedures, explaining how the HPLC/UV/MS analysis method works in the identification of PAH. We then summarize the results we have obtained by HPLC/UV/MS analysis of the supercritical pyrolysis products of two of our model fuels, 1-methylnaphthalene and toluene—presenting the PAH formation reaction mechanisms that the HPLC/UV/MS results have helped us to devise. The results of the HPLC/UV/MS analyses of one of the UTRC samples from a Fischer-Tropsch synthetic jet fuel are then presented, followed by a summary of all of the results presented in this report. Finally, we list the publications and conference presentations to which results from the HPLC/UV/MS have contributed.

Experimental Equipment and Techniques

Since most of the products analyzed with the new HPLC/UV/MS come from our supercritical pyrolysis experiments with model fuels, here we describe the reactor used in these experiments. We then describe the instruments and techniques used in the analysis of these and other product mixtures supplied to us from the Air Force Research Laboratory and United Technologies Research Center.

Reactor System

The supercritical fuel pyrolysis experiments are conducted in the isothermal, isobaric reactor designed expressly for such purposes by Davis [8] and used by Stewart [9,10] in the AFOSR-sponsored research program supervised by Professor Irvin Glassman at Princeton University. Upon his retirement, Professor Glassman made the reactor available to us, and we have used it for supercritical fuel pyrolysis research over the last several years.

The reactor system [6,11] is illustrated in Figure 1. Prior to an experiment, liquid fuel is sparged with nitrogen for three hours [9] to remove any dissolved oxygen that could introduce auto-oxidative effects [12]. The sparged fuel is then loaded into a high-pressure pump, which delivers the fuel to the reactor, as shown in Figure 1. The reactor itself is a silica-lined stainless-steel coil of 1-mm i.d., 1.59-mm o.d. capillary tubing. (The silica lining prevents wall-catalyzed

deposit formation that occurs with unlined stainless steel [8,9,12].) The reactor coil is immersed in a temperature-controlled fluidized-alumina bath, which ensures isothermality throughout the reactor length. As indicated in Figure 1, the entrance and exit lines of the reactor are passed through a water-cooled (25 °C) heat exchanger to ensure a controlled thermal history and residence time. Exiting the heat exchanger, the quenched reaction products pass through a stainless-steel filter (hole size, 10 μm) and on to a high-pressure valve, for liquid product collection in the sample loop. Gaseous products are collected in a Teflon sampling bag following the high-pressure valve. A dome-loaded back-pressure regulator, downstream of the valve, controls the system pressure, to within ± 0.2 atm, up to a maximum of 110 atm.

Reactor residence time is varied by changing the length of the reactor coil or the flowrate. The reactor system is capable of operating at temperatures up to 585 °C, pressures up to 110 atm, and residence times up to several minutes. As documented by Davis [8] and Stewart [9], the reactor has been designed to meet Cutler's [13] and Lee's [14] criteria for idealization as plug flow, with regard to species concentration profiles. The resulting radially uniform species concentrations, coupled with the reactor's constant-temperature and constant-pressure operation, render this reactor ideal for supercritical pyrolysis kinetics experiments.

Product Analysis

At the conclusion of a pyrolysis experiment, the gaseous reaction products are removed and injected into an Agilent Model 6890N gas chromatograph (GC) with a flame-ionization detector (FID), for analysis of light-hydrocarbon gases. The liquid products are removed from the high-pressure collection valve and transferred to a vial. Most of the liquid product mixture is reserved for analysis by high-pressure liquid chromatography (HPLC), but a 20- μL aliquot of the liquid product mixture is removed for injection onto an Agilent Model 6890 GC with a FID, in conjunction with an Agilent Model 5973 mass spectrometer (MS). The GC/FID/MS instrument is used to quantify the 1- to 2-ring (and sometimes 3- or 4-ring) liquid aromatic products—all of

which are identified by matching retention times and mass spectra with those of reference standards.

The portion of the liquid product mixture reserved for HPLC analysis is concentrated in a Kuderna-Danish apparatus and exchanged, under nitrogen, into 200 μ L of dimethylsulfoxide, a solvent compatible with the solvents used in the HPLC method employed for PAH analysis. During the concentration and solvent-exchange procedure, portions of the more volatile aromatics, such as the 1- and 2-ring species, are lost to vaporization; hence these lighter aromatic products are quantified by gas chromatographic analysis, as described above.

For analysis of the large aromatic products (≥ 3 rings) by HPLC, a 20- μ L aliquot of the product/dimethylsulfoxide solution is injected onto an Agilent Model 1100 high-pressure liquid chromatograph, coupled to a diode-array ultraviolet-visible (UV) absorbance detector in series with a mass spectrometer (MS)—the HPLC/UV/MS instrument purchased through this DURIP grant. The HPLC separation method utilizes a reversed-phase Restek Pinnacle II PAH octadecylsilica column (particle size, 5 μ m; inner diameter, 4.6 mm; and length, 250 mm). A time-programmed sequence of solvents—acetonitrile/water, acetonitrile, and dichloromethane—is pumped through the HPLC column, and the PAH product components elute in the order of increasing molecular size. An alternative solvent program—using methanol/water, methanol, and dichloromethane—is employed in some cases, to optimize separation of the large PAH. UV absorbance spectra are taken every 0.25 sec of the separated components as they exit the HPLC column. The diode-array UV detector monitors absorbance from 190 to 520 nm, the full range of UV wavelengths over which PAH absorb. Mass spectra are taken of the components after they leave the UV detector. The MS employs atmospheric-pressure photo ionization and simultaneously monitors two ranges of mass-to-charge ratio: 75 to 500 and 273 to 550, with a cycle time of 1.02 sec.

The mass spectrum establishes the C_xH_y formula of the PAH, its molecular mass, and whether there are any substituent groups like methyl attached to the aromatic structure. The UV spectrum establishes the exact aromatic structure of the PAH, so for unsubstituted PAH, the UV spectrum

alone is sufficient to establish the exact isomer-specific identity. If a PAH has an alkyl substituent, the UV spectrum looks almost exactly like that of the parent PAH, only shifted a few nm to higher wavelength—the position and length of the substituent dictating the details of the shift [15,16]. Therefore, for large PAH, which have a multitude of sites at which substituents can be located, one must have reference standards of all possible positional isomers in order to be certain of the exact position of the alkyl substituent—a condition rarely met. Consequently, for each of the alkylated PAH products of ≥ 5 rings reported in the Results and Discussion section of this Report, the exact structure of the aromatic portion of the PAH is known (from the UV spectrum); only the exact position of the alkyl group is uncertain.

PAH products from the supercritical fuel pyrolysis experiments are identified by matching HPLC retention times, mass spectra, and UV absorbance spectra with those of our PAH reference standards, which include both commercially available compounds as well as PAH that have been specially synthesized for our identification efforts. In some cases, in which reference standards are not available, product identities are established by matching UV spectra with those published in the literature for those compounds. Quantification of the identified PAH comes from extensive calibration of the HPLC instrument with reference standards, taking into account nonlinearities in the response of diode-array detectors at high analyte concentrations [17].

Since the number of possible PAH structures grows exponentially with ring number [16], the HPLC/UV/MS technique is particularly well suited for analyzing the large PAH molecules that are precursors to fuel-line carbonaceous solids. The HPLC separates each product component; the mass spectrum narrows the field of possible component identities to a particular C_xH_y isomer group; the fingerprint UV spectrum then permits the designation of the exact molecular structure of the product component. The power of the HPLC/UV/MS method—in the analysis of supercritical pyrolysis products of both model fuels as well as a synthetic jet fuel—is illustrated in the Results and Discussion section of this Report. It should be emphasized that the HPLC/UV/MS means of analyzing large PAH is a very highly specialized technique—a capability of only a few laboratories in the world.

Illustration of How the HPLC/UV/MS Technique Works

The HPLC/UV/MS separation and identification method is illustrated in Figure 2, an HPLC chromatogram of a mixture of PAH reference standards. The peaks in the chromatogram represent individual components of the original mixture, which the HPLC has separated by the flow of solvents through the HPLC column. For any given component, such as the one eluting at 44.4 minutes in Figure 2, the HPLC/UV/MS instrument's computer records the component's mass spectrum and UV spectrum as the component is eluting from the HPLC column. The component eluting at 44.4 min in Figure 2, for example, has the mass spectrum that is the left inset of Figure 2 and the UV spectrum that is the right inset of Figure 2. For PAH subjected to atmospheric-pressure photo ionization in our HPLC/UV/MS system, the primary ion exhibited by the mass spectrum is dependent on the solvent running through the HPLC at the time the component is eluting [18]. If the solvent is acetonitrile, such as is the case in Figure 2, the primary ion is at $m/z = M$, the molecular mass of the PAH. If the solvent is dichloromethane or methanol, such as is the case in some examples to be illustrated in the Results and Discussion, proton transfer from the solvent [18,19] causes the primary ion in the PAH mass spectrum to be at $m/z = M+1$. In either case, the mass spectrum establishes the C_xH_y formula of the separated PAH component— $C_{22}H_{12}$ (from $M = 276$) for the component eluting at 44.4 min in Figure 2. The UV spectrum of this same component, shown as the black curve in the right inset of Figure 2, establishes exactly which $C_{22}H_{12}$ PAH this component is—benzo[ghi]perylene in this case, since the component's UV spectrum matches that of the reference standard of benzo[ghi]perylene, shown in red. The identity of the mixture component eluting at 44.4 min in Figure 2, is thus unequivocally established as benzo[ghi]perylene.

Since benzo[ghi]perylene is readily available as a reference standard from commercial sources, its identification would have been very straight forward simply from its UV absorbance spectrum, and the mass spectrum would not have been necessary. However, for larger-ring-number PAH, for which the number of possible isomers is huge (hundreds or even thousands) and reference standards are scarce, the mass spectrum provides information critically helpful to PAH

identification, since it narrows the field of possible candidates down to a particular isomer family. Examples are demonstrated in the Results and Discussion section to follow.

Results and Discussion

In order to demonstrate the kind of results we have been able to obtain from the HPLC/UV/MS instrument purchased on the DURIP grant, in this section we describe results from experiments conducted with two model fuels, under our current AFOSR Grant FA9550-04-1-0005, as well as results on a synthetic jet fuel of interest to the Air Force, the Fischer-Tropsch fuel S-8. The model fuel results come from our experiments (in the reactor of Figure 1) with 1-methylnaphthalene, a two-ring aromatic component of jet fuel [20], and toluene, a single-ring aromatic component of jet fuel [20]. The results on the Fischer-Tropsch fuel come from our compositional analyses of certain stressed synthetic jet fuel samples provided to us by Dr. He Huang at United Technologies Research Center, at the instigation of Dr. Tim Edwards at AFRL.

Model Fuel Experiments with 1-Methylnaphthalene

Figure 3 presents the HPLC chromatogram of the aromatic products from 1-methylnaphthalene (critical temperature, 499 °C; critical pressure, 36 atm) pyrolysis at 585 °C, 110 atm, and 140 sec. In addition to that of 1-methylnaphthalene itself (unreacted fuel), Figure 3 displays the structures of the 37 individual two- to seven-ring PAH products that have been identified by HPLC/UV/MS, as well as the molecular masses of the eight- and nine-ring PAH products whose exact identities are not yet known. The clusters of peaks representing the > 30 binaphthyl products are also labelled in Figure 3.

Fifteen of the PAH of ≥ 5 rings in Figure 3 have never before been identified as products of 1-methylnaphthalene pyrolysis or combustion, so a paper providing the HPLC, UV, and MS evidence documenting the identifications of these PAH is currently in preparation [21]. The mass

and UV spectra establishing the identities of two of these new products, the $C_{24}H_{14}$ naphtho[2,1-*a*]pyrene and the $C_{21}H_{14}$ dibenzo[*a,i*]fluorene, are presented in Figures 4 and 5, respectively. Figure 4a establishes that the product component with elution time 63.3 min in Figure 3 is a $C_{24}H_{14}$ PAH; Figure 4b shows that this $C_{24}H_{14}$ component is specifically naphtho[2,1-*a*]pyrene, as its UV spectrum matches that of our reference standard for that compound. Figure 5a establishes that the product component with elution time 40.4 min in Figure 3 is a $C_{21}H_{14}$ PAH; Figure 5b shows that this $C_{21}H_{14}$ component is specifically dibenzo[*a,i*]fluorene, as its UV spectrum matches that published [22,23] for this compound.

It is worth noting that since a reference standard of dibenzo[*a,i*]fluorene is not available, since its UV spectrum was not among our collection, and since we had never before encountered it as a product from any fuel—our ability to identify it, and the seven other products of the $C_{21}H_{14}$ family (the green structures of Figure 3) was tremendously facilitated by the acquisition of the HPLC/UV/MS instrument. Once we got the HPLC/UV/MS, we were able to determine from the mass spectra that these product components were $C_{21}H_{14}$ PAH and methylated $C_{21}H_{14}$ PAH. We thus began a search of the chemical literature for UV spectra of $C_{21}H_{14}$ PAH, and it was this search that yielded the published UV spectra [22-25] of the dibenzofluorenes and enabled us to identify the eight products in this family as well as establish which dibenzofluorenes were not products.

The many product PAH of Figure 3 fall into six classes, as listed in Table 1: Class 1, naphthalene and the alkylated naphthalenes, accounting for 46% and 12%, respectively, of the PAH products and eluting in the 13- to 25-minute retention-time range of the HPLC chromatogram of Figure 3; Class 2, the bi-naphthyls, accounting for 39% of the PAH products and eluting from 26 to 38 min; Class 3 (structures shown in blue), the $C_{20}H_{12}$ 5-ring PAH and their methyl derivatives, accounting for 0.071% of the PAH products; Class 4 (structures shown in

green), the dibenzofluorenes, accounting for 1.6% of the PAH products; Class 5 (structures shown in red), the $C_{22}H_{14}$ 5-ring PAH, accounting for 0.61% of the PAH products; and Class 6 (structures shown in black), the 6-ring and 7-ring PAH, accounting for 0.5% of the PAH products and eluting after 72 minutes. Our paper recently accepted to the Thirty-First International Combustion Symposium [20] describes each of the product groups in detail, in addition to the radical reaction pathways leading to their formation in the supercritical 1-methylnaphthalene pyrolysis environment. The key findings of that paper [11] are summarized here in Table 1 and are described in the following. Useful in the ensuing discussion is an awareness of the various bond dissociation energies (BDEs) associated with the 1-methylnaphthalene molecule. The various BDE values [26,27], depicted in Figure 6, show that the methyl C-H bond is the bond of lowest BDE. Therefore, in our analyses of the radical reaction pathways for the 1-methylnaphthalene pyrolysis environment, we presume, as have others [28,29], that the initial source of radicals is homolysis of the methyl C-H bond, to yield 1-naphthylmethyl radical and hydrogen atom.

As shown in Table 1, the first group of supercritical 1-methylnaphthalene pyrolysis products are those of Class 1: naphthalene, 1-ethylnaphthalene, 2-methylnaphthalene, all ten of the dimethylnaphthalenes, and one C_3 -substituted naphthalene. As depicted in Table 1, the Class 1 products result from either displacement of methyl by hydrogen or vice versa. What the structures of the Class 1 products reveal is that within the supercritical 1-methylnaphthalene pyrolysis environment, it is possible to break the methyl C-H bond (BDE, 85.1 kcal/mole [26]), the methyl-aryl C-C bond (BDE, 103.8 kcal/mole [26]), and the aryl C-H bond (BDE, 112.2 kcal/mole [26]). Since we find no single-ring aromatics among our products and since the gaseous hydrocarbon products we observe (90 % methane, 5% ethane, and the balance C_3 to C_4 alkanes, with only a trace of ethylene—and no acetylene) can all come from methyl and hydrogen—we see that the only kind of bond that appears not to be broken in this reaction

environment is the aromatic C-C bond (BDE, 122.3 kcal/mole [27]). We could thus expect the larger aromatic products in this reaction environment to be formed by different combinations of methyl, hydrogen, naphthalene, and 1-methylnaphthalene radicals and molecules—forming bonds in ways that preserve the 2-ring aromatic units of the reacting naphthalene and methylnaphthalene entities.

The first evidence that this hypothesis is indeed the case comes from the structures of the Class 2 products, the bi-naphthyls and methylated bi-naphthyls, the large cluster of peaks between 26 and 38 min in Figure 3. Examples of some of the > 30 Class 2 products are shown in the left-most column of Table 1. As indicated in the middle column of Table 1, the Class 2 products are formed by displacement of 1-methylnaphthalene's methyl or one of its hydrogens by naphthylmethyl, methylnaphthyl, or naphthyl radical. What we see from the structures of the Class 2 products is that the two-ring naphthalene units stay intact as the various methyl and hydrogen displacements take place on the periphery of the structure.

The next group of 1-methylnaphthalene products in Table 1 are those of Class 3, the five-ring $C_{20}H_{12}$ PAH. These Class 3 products result from the cyclodehydrogenation of the Class 2 products, as illustrated in Table 1. No breaking of the aromatic C-C bond is involved in the process, so the intactness of the two participating 2-ring naphthalene units is preserved in the resulting five-ring fused PAH structures. We know from our HPLC/UV/MS analyses that other $C_{20}H_{12}$ isomers of the Class 3 products, such as the two compounds shown in the right-most column of Table 1 (in the Class 3 section), are not produced in the supercritical 1-methylnaphthalene reaction environment, and their absence is not a surprise since they cannot be formed from two naphthalene units in a way that would preserve the intactness of the naphthalene units.

The second group of five-ring products of 1-methylnaphthalene, also pictured in Table 1, are those of Class 4, the $C_{21}H_{14}$ dibenzofluorenes and their methyl derivatives. As shown in Table 1, the dibenzofluorenes are formed by 1-naphthylmethyl displacement of an aryl H of either naphthalene or a methylnaphthalene, followed by dehydrogenation. As in the case of the Class 3 products, the structures of the $C_{21}H_{14}$ PAH of Class 4 reflect the intactness of the two naphthalene units involved in their construction, and no $C_{21}H_{14}$ isomers that involve other building units such as 1-ring/3-ring combinations are observed. The Class 4 products exhibit an additional level of selectivity in that: $C_{21}H_{14}$ PAH whose formation would require 2-naphthylmethyl radical addition to a “2” position of naphthalene are not made in this 1-methylnaphthalene reaction environment, in which 1-naphthylmethyl would be in much greater abundance than its “2” counterpart.

The third group of five-ring products of supercritical 1-methylnaphthalene pyrolysis, also listed in Table 1, are the $C_{22}H_{14}$ PAH composing Class 5. As shown in Table 1, these $C_{22}H_{14}$ PAH are produced by the addition of 1-naphthylmethyl radical to either 1-methylnaphthalene or 2-methylnaphthalene, followed by dehydrogenation. As in the case of the other Classes of five-ring products, we see that the four Class 5 $C_{22}H_{14}$ products all preserve the intactness of the two 2-ring naphthalene units involved in their formation. Because our HPLC/UV/MS technique enables us to see which isomers of the 12 possible $C_{22}H_{14}$ PAH are present as well as which are not, we can see that the $C_{22}H_{14}$ Class 5 products exhibit several degrees of selectivity: (1) $C_{22}H_{14}$ PAH whose structures do not contain two intact naphthalene units are not observed. (2) $C_{22}H_{14}$ PAH whose construction involves the combination of a 2-naphthylmethyl radical and a 2-methylnaphthalene molecule—but no involvement of the “1” counterparts—are not observed. (3) For a given sequence of steps, products constructed from 1-naphthylmethyl radical and 1-methylnaphthalene molecule are produced in higher abundance than are those constructed from 1-naphthylmethyl radical and 2-methylnaphthalene.

Product selectivity is particularly evident among the last set of 1-methylnaphthalene products listed in Table 1, those comprising Class 6: the 6- and 7-ring PAH eluting between 63 and 80 min in Figure 3, whose structures are shown in black. None of the Class 6 products has ever before been reported as a product of 1-methylnaphthalene pyrolysis or combustion.

As Figure 3 reveals, the highest-yield Class 6 product is the $C_{24}H_{14}$ naphtho[2,1-*a*]pyrene, whose formation, we propose, occurs as depicted in the top row of the second column of Table 1, in the Class 6 section. As shown in the second row of the same column, naphtho[2,3-*a*]pyrene, the other $C_{24}H_{14}$ product we observe, would form according to the same sequence, but with the initial methyl additions occurring to the methyl group of 2-methylnaphthalene instead of to 1-methylnaphthalene. The yield of naphtho[2,3-*a*]pyrene is more than two orders of magnitude lower than that of naphtho[2,1-*a*]pyrene—reflecting the much lower level of 2-methylnaphthalene in our system, relative to 1-methylnaphthalene. We know from our HPLC/UV/MS analyses that only one other $C_{24}H_{14}$ PAH (as yet unidentified) exists among our 1-methylnaphthalene products, and that one is also only in trace levels.

The fact that one particular 6-ring compound, naphtho[2,1-*a*]pyrene, is in such high yield (comparable to those of some of the more abundant di-methylnaphthalenes) is truly remarkable, especially when one considers that naphtho[2,1-*a*]pyrene belongs to the $C_{24}H_{14}$ PAH family of which there are 65 possible isomers [30]. Once again we witness the extreme selectivity of the products formed in the supercritical 1-methylnaphthalene pyrolysis reaction environment. Our paper [11] provides the details as to why the other $C_{24}H_{14}$ PAH are not formed in this reaction environment; some examples are highlighted here, in the last column of Table 1, under the Class 6 section. The long and short of it is that—just as we observed for the 5-ring PAH products—the 6-ring products which are formed are those whose structures preserve the intactness of the parent

two 2-ring naphthalene units, whose reaction pathways involve the species most abundant in the reaction environment, and whose formation involves bond breakage at the sites of lowest BDE.

The bottom row of Table 1 reveals the remaining Class 6 product: the 7-ring dibenzo[*cd,lm*]perylene, whose formation pathway runs along the same lines as those for the 6-ring PAH but with two extra methylations required. As with the 5- and 6-ring PAH, a high degree of selectivity is exhibited by the 7-ring PAH, as dibenzo[*cd,lm*]perylene is the only $C_{26}H_{14}$ PAH product detected in the supercritical 1-methylnaphthalene pyrolysis products.

In addition to the 2- to 7-ring PAH products listed in Table 1, Figure 3 shows seven unidentified peaks: six labelled “402” and one labelled “426,” in accordance with the molecular masses determined from the mass spectra for those components. In order to learn more about these 8- and 9-ring products (which may be key precursors to carbonaceous solids), the product mixture portrayed in Figure 3 has been subjected to another HPLC/UV/MS analysis employing the solvents methanol and dichloromethane, which optimize HPLC separation of the high-ring-number PAH. The end segment of the resulting HPLC chromatogram is pictured in Figure 7, which shows two of the Class 6 products from Figure 3 as well as eleven unsubstituted 8- and 9-ring PAH products: six 8-ring $C_{32}H_{18}$ of molecular mass 402 and five 9-ring $C_{34}H_{18}$ of molecular mass 426. There are also five molecular-mass 416 products which, we know from their mass and UV spectra, are methylated versions of two of the 8-ring $C_{32}H_{18}$ products.

In the supercritical 1-methylnaphthalene pyrolysis environment, the 8-ring $C_{32}H_{18}$ PAH can be constructed from 1-naphthylmethyl radical reacting with naphthalene and 1-methylnaphthalene; the $C_{34}H_{18}$ PAH can be constructed from 1-naphthylmethyl radical, methyl, and two 1-methylnaphthalenes. Of the 287 theoretically possible benzenoid $C_{32}H_{18}$ PAH and the 333 theoretically possible benzenoid $C_{34}H_{18}$ PAH [31], there are, respectively, only 13 [32-37] and 12 isomers [37-41] for which UV spectra have been published, and none of these published UV

spectra match any of the spectra of our $C_{32}H_{18}$ and $C_{34}H_{18}$ 1-methylnaphthalene products. Even if one imposes the restriction—based on the findings of our 2- to 7-ring products—that the 8- and 9-ring PAH products must reflect the preservation of the three 2-ring naphthalene units that could be involved in their construction, the field of possible $C_{32}H_{18}$ and $C_{34}H_{18}$ benzenoid PAH candidates is only “narrowed down” to, respectively, 83 and 189 isomers—still some rather daunting numbers since only 6 of the 83 and 2 of the 189 have published UV spectra.

Nevertheless, the HPLC/UV/MS instrument, in conjunction with Annellation Theory [16,37], has enabled us to identify the latest-eluting molecular-mass 426 component in Figure 7. The very long HPLC elution time (174 min) itself provides a very important clue to the identity of this product component: because of its very long elution time, this PAH product has to be planar and has to have a high length-to-breadth ratio [42-44]. This late-eluting $C_{34}H_{18}$ PAH product, we believe, is benzo[*cd*]phenanthro[1,2,3-*lm*]perylene, whose structure is shown in red in Figures 8 and 9, along with the UV spectral evidence supporting this product’s identification. No reference standard or published UV spectrum of benzo[*cd*]phenanthro[1,2,3-*lm*]perylene exists, so—unlike Figures 4b and 5b, which show the UV spectra of the product components with those of their respective reference standards—Figures 8 and 9 show the UV spectrum of the $C_{34}H_{18}$ product component eluting at 174 min (which we are deducing to be benzo[*cd*]phenanthro[1,2,3-*lm*]perylene), along with the published UV spectra of two of benzo[*cd*]phenanthro[1,2,3-*lm*]perylene’s benzologues: one with one ring less, the $C_{30}H_{16}$ benzo[*cd*]naphtho[1,2,3-*lm*]perylene [16], shown in black in Figure 8; and one with one ring more, the $C_{36}H_{18}$ teropyrene [45], shown in black in Figure 9. The extreme similarity between the two spectra of Figure 8 establishes that the structure of the $C_{34}H_{18}$ product component eluting at 174 min in Figure 7 has to resemble very closely the structure of benzo[*cd*]naphtho[1,2,3-*lm*]perylene, the $C_{30}H_{16}$ shown in

black in Figure 8. The line of reasoning leading to our deduction of the exact structure of the $C_{34}H_{18}$ product is detailed in the following.

Consistent with the similarities of the three molecular structures drawn in Figures 8 and 9, all three of the UV spectra in the two figures exhibit the same basic shapes and patterns, especially in the relative heights of the peaks in the p band (the three highest-wavelength peaks). The three molecules are not the same, however, so there are differences between the spectra in Figures 8 and 9, primarily in the positions (wavelengths) of the various spectral peaks: the red spectrum of the 9-ring compound in Figure 8 is very similar (in the β and p bands) to the black spectrum of the 8-ring compound, but there are some differences in the β' band; the black spectrum of the 10-ring compound in Figure 9 is shifted substantially, relative to the red spectrum of the 9-ring compound. The spectral similarities and differences among the benzologues of Figures 8 and 9 are fully consistent with the assignment of the 9-ring product's identity as benzo[*cd*]phenanthro[1,2,3-*lm*]perylene, however, and can be explained by Annellation Theory [16,37,46], as detailed below.

One tenet of Annellation Theory [16,37,46] is that the addition of a ring to a bay region of a PAH molecule causes the overall appearance of the UV spectrum to be preserved but shifts the spectrum to higher wavelengths (~ 10 nm for the β band and 10s of nm for the p band). The 9- and 10-ring PAH of Figure 9 conform exactly to this behavior. The structure of teropyrene differs from that of benzo[*cd*]phenanthro[1,2,3-*lm*]perylene by the addition of a ring to a bay region, and its spectrum, relative to that of the 9-ring benzologue, is shifted ~ 15 nm in the β band and 50-60 nm in the p band.

A second tenet of Annellation Theory [16,37,46] states that when addition of a ring to a PAH molecule (a) occurs to a ring with one or more isolated π bonds and (b) results in the addition of an aromatic sextet, the effects on the β and p bands of the UV spectrum are extremely minimal

(but the β' band may be shifted). The 8- and 9-ring PAH of Figure 8 conform exactly to this behavior. The structure of benzo[*cd*]phenanthro[1,2,3-*lm*]perylene differs from that of benzo[*cd*]naphtho[1,2,3-*lm*]perylene by the addition of an aromatic sextet to a ring with two isolated *pi* bonds, and the β and *p* bands of the UV spectra of the two compounds are extremely similar. The β' band of the 9-ring compound's spectrum is shifted ~4 nm to the right, relative to that of the 8-ring compound.

In order to confirm that the 9-ring product component eluting at 174 min in Figure 7 is in fact benzo[*cd*]phenanthro[1,2,3-*lm*]perylene and cannot be any other $C_{34}H_{18}$ benzologue of benzo[*cd*]naphtho[1,2,3-*lm*]perylene (the 8-ring structure of Figure 8), we consider the structures of all of the benzenoid molecules of formula $C_{34}H_{18}$ that can result by addition of a ring to benzo[*cd*]naphtho[1,2,3-*lm*]perylene. The nine possible $C_{34}H_{18}$ structures are shown in Figure 10, along with that of benzo[*cd*]naphtho[1,2,3-*lm*]perylene itself, the “parent” 8-ring compound in the center of Figure 10. Immediately we can see that five of the nine possibilities—those in green, resulting from ring fusion to the *e*, *i*, *p*, *t*, or *x* sides of benzo[*cd*]naphtho[1,2,3-*lm*]perylene—cannot be our 9-ring $C_{34}H_{18}$ product since each of these five has a “cove” region that makes the molecular structure nonplanar [16]. The nonplanarity would cause these species to elute much earlier in Figure 7 than the 174 min of our $C_{34}H_{18}$ product. Nonplanarity also causes broadening of bands in the UV spectra—as well as attenuation of spectral peaks and raising of spectral valleys [16]—so the $C_{34}H_{18}$ product component spectrum in Figures 8 and 9 could not correspond to any of the five nonplanar structures (in green) in Figure 10.

To assess the remaining four possible $C_{34}H_{18}$ PAH of Figure 10, we next employ a corollary to the second tenet of Annellation Theory [16,37,46], which states that if ring addition to a ring with one or more isolated *pi* bonds does not result in the addition of a sextet (*i.e.*, a violation of condition (b) above), then the UV spectrum is altered substantially: the *p* band is shifted 10s of

nm; the β band shifts and is altered in shape. In Figure 10, fusion of a ring to the *o* side of benzo[*cd*]naphtho[1,2,3-*lm*]perylene corresponds to just such a case, so the blue structure at the top of Figure 10 is eliminated as a candidate for our C₃₄H₁₈ product eluting at 174 min in Figure 7.

In our consideration of the final three C₃₄H₁₈ candidates in Figure 10, we turn to a third tenet of Annellation Theory [16,37,46], which states that addition of a ring to an aromatic sextet preserves the basic appearance of the UV spectrum but shifts it to substantially higher wavelengths (by ~30 nm for the highest-wavelength peak of the *p* band), provided that the resulting molecule has the same number of aromatic sextets as the parent molecule. Fusion of a ring to either the *a* or *b* side of benzo[*cd*]naphtho[1,2,3-*lm*]perylene exemplifies this case, so the UV spectra of the two structures shown in turquoise at the bottom of Figure 10 would be substantially different from that of benzo[*cd*]naphtho[1,2,3-*lm*]perylene. The third tenet of Annellation Theory thus rules the two turquoise structures out as possible candidates for the C₃₄H₁₈ product eluting at 174 min in Figure 7.

We see that the only one of the nine C₃₄H₁₈ possibilities that meets all of the criteria—molecular formula C₃₄H₁₈, planarity, high length-to-breadth ratio, UV spectrum similar to that of the 8-ring benzologue and consistency with the tenets of Annellation Theory—is benzo[*cd*]phenanthro[1,2,3-*lm*]perylene, shown in red in Figures 8, 9, and 10. We also note that benzo[*cd*]phenanthro[1,2,3-*lm*]perylene's structure reflects the preservation of three intact 2-ring naphthalene units—just as the structures of the 5- to 7-ring products in Figure 3 reflect the preservation of two intact 2-ring naphthalene units. Benzo[*cd*]phenanthro[1,2,3-*lm*]perylene is thus the C₃₄H₁₈ PAH product of supercritical 1-methylnaphthalene pyrolysis that elutes at 174 min in Figure 7. This PAH has never before been identified as a product of any fuel under any condition. In fact, **benzo[*cd*]phenanthro[1,2,3-*lm*]perylene has never before been reported in the scientific literature.** This is the first documentation of this molecule's existence.

Figure 11 presents the reaction scheme for the formation of benzo[*cd*]phenanthro[1,2,3-*lm*]perylene in the supercritical 1-methylnaphthalene pyrolysis environment. Methylation of the methyl group of 1-methylnaphthalene forms 1-ethylnaphthalene (a product in Figure 3), which then reacts with two 1-naphthylmethyl radicals, as shown in Figure 11, and undergoes a series of dehydrogenation and ring-closure steps to form benzo[*cd*]phenanthro[1,2,3-*lm*]perylene. Just as the reaction schemes of Table 1—forming the 5-, 6-, and 7-ring products of Figure 3—involve the combination of two naphthalene or 1-methylnaphthalene molecules or radicals and methyl, the scheme to form the 9-ring benzo[*cd*]phenanthro[1,2,3-*lm*]perylene in Figure 11 involves combination of three naphthalene or 1-methylnaphthalene molecules or radicals and methyl. We expect that the other C₃₄H₁₈ products of Figure 7, not yet identified, would be formed by reactions very similar to the scheme of Figure 11 but with aryl-alkyl bonds forming at different aryl positions during the sequence, resulting in different isomeric configurations of 9-ring structures.

The fact that—out of the hundreds of possible 8- and 9-ring PAH—only six C₃₂H₁₈ and five C₃₄H₁₈ isomers exhibit prominence in Figure 7 suggests that a high degree of product selectivity is in effect for these 8- and 9-ring products, just as it has been demonstrated in the 5-, 6-, and 7-ring PAH products of supercritical 1-methylnaphthalene pyrolysis. Even though the exact identities of most of these 8- and 9-ring products have not yet been determined, their presence, along with their suggested selectivity, serve as evidence that the types of reaction mechanisms outlined in Table 1—for the combination of two naphthalene and methylnaphthalene entities in the formation of 5- to 7-ring PAH—apply to the combination of three and more such entities in the formation of larger-ring-number PAH and eventually carbonaceous solids. Without the HPLC/UV/MS instrument, it would have been extremely difficult to establish these findings so irrefutably.

Model Fuel Experiments with Toluene

The results described above illustrate the usefulness of the HPLC/UV/MS analysis technique in discerning the structures of large PAH products and in determining the reaction pathways responsible for large PAH formation from the 2-ring aromatic jet fuel component 1-methylnaphthalene. We now highlight some of the results of applying this same analytical technique to the supercritical pyrolysis products of the 1-ring aromatic jet fuel component toluene (critical temperature, 319 °C; critical pressure, 41 atm).

Figure 12 presents the HPLC chromatogram of supercritical toluene pyrolysis products from experiments in the reactor of Figure 1, at conditions of 535 °C, 100 atm, and 140 sec. As in the case of the 1-methylnaphthalene products, the HPLC/UV/MS instrument purchased on DURIP funds has greatly aided the identification of the products of toluene, particularly the large PAH, which are precursors to carbonaceous solids in the supercritical fuel pyrolysis environment. A good case in point is the set of six 8-ring $C_{28}H_{14}$ PAH whose structures are shown in red in Figure 12. As indicated in Table 2 (a listing of all the possible $C_{28}H_{14}$ benzenoid PAH), we have identified two of the $C_{28}H_{14}$ products of Figure 12—benzo[*a*]coronene and benzo[*pqr*]naphtho[8,1,2-*bcd*]perylene—by matching the UV spectra of the product components with those of the specially synthesized [39,47-49] reference standards in our collection. Two others—phenanthro[5,4,3,2-*efghi*]perylene and benzo[*cd*]naphtho[8,1,2,3-*fghi*]perylene—we have identified by establishing the components' molecular formula from their mass spectra and then matching the components' UV spectra with those published [50-52] for the respective PAH reference standards. The remaining two $C_{28}H_{14}$ products—benzo[*ghi*]naphtho[8,1,2-*bcd*]perylene and tribenzo[*cd,ghi,lm*]perylene—we have identified [46,53] through the combination of HPLC retention time data (which relate to molecular length-to-breadth ratios), mass spectra, UV spectra, and Annellation Theory—just as we have illustrated in the previous section for the identification of the $C_{34}H_{18}$ benzo[*cd*]phenanthro[1,2,3-*lm*]perylene as a product of the supercritical pyrolysis of

1-methylnaphthalene. It is worth noting that prior to acquiring the HPLC/UV/MS, the only two of the $C_{28}H_{14}$ products that we were able to identify were the first two listed in Table 2, the ones for which we had the actual reference standards.

As in the case of the 1-methylnaphthalene work, the HPLC/UV/MS instrument has enabled us to determine not only which isomers of a given PAH family are products of supercritical toluene pyrolysis but also those that are not. In the case of the $C_{28}H_{14}$ PAH, we have been able to establish that bisanthene, the second-to-last $C_{28}H_{14}$ benzenoid PAH listed in Table 2, is not a product of supercritical toluene pyrolysis, as its published UV spectrum [37] does not match the UV spectrum of any of the six $C_{28}H_{14}$ components in the toluene product mixture. In addition, Annellation Theory has permitted us to establish [46] from the predicted UV spectrum, that naphthaceno[3,4,5,6,7-*defghij*]naphthacene, the last entry of Table 2, is also not among the supercritical toluene pyrolysis products.

Figure 13, extracted from our recent paper [54], illustrates how the six $C_{28}H_{14}$ products in Figure 12 and Table 2 are formed in the supercritical toluene pyrolysis environment. As in the case of 1-methylnaphthalene, the products of supercritical toluene pyrolysis show that the aromatic C-C bond is not broken in this reaction environment; so, as Figure 13 shows, the PAH are “built” from sequential additions of benzyl, methyl, and/or phenyl radicals—all plentiful in the toluene pyrolysis environment—followed by dehydrogenation. Just as the major building blocks for PAH formation from supercritical 1-methylnaphthalene pyrolysis have been shown to be 1-naphthylmethyl radical, methyl radical, 1-methylnaphthalene, and naphthalene—Figure 13 reveals that the building blocks for PAH formation from supercritical toluene pyrolysis are the exact analogues: benzyl radical, methyl radical, toluene, and benzene (or phenyl radical). Another similarity in the results for the two aromatic fuels is that: just as the HPLC/UV/MS analyses of the 1-methylnaphthalene products have helped to provide mechanistic insight into

why certain 5- to 7-ring PAH are formed and why others are not, so have the HPLC/UV/MS analyses of the toluene products helped to provide mechanistic insight into why certain PAH are formed and others are not in the supercritical toluene pyrolysis environment: Figure 13 shows that all six of the $C_{28}H_{14}$ products of supercritical toluene pyrolysis are produced via pathways that involve intermediates that are fully aromatic benzenoid structures that themselves are observed products in Figure 12. Figure 14 demonstrates that attempts to form—from the benzyl, methyl, and phenyl building blocks in our system—the two $C_{28}H_{14}$ PAH of Table 2 that are known not to be among our products would involve not-fully-aromatic intermediates that we know from our HPLC/UV/MS analyses are also not present in the product mixture. There are thus mechanistic reasons why certain large PAH are made and why certain others are not in the supercritical toluene pyrolysis environment—just as we have seen for the supercritical 1-methylnaphthalene pyrolysis environment.

The alternate HPLC solvent program responsible for the 1-methylnaphthalene products chromatogram excerpted in Figure 7 has also been applied to the products of supercritical toluene pyrolysis, yielding the HPLC chromatogram whose end portion appears in Figure 15. The chromatogram reveals the presence of seven 10-ring $C_{34}H_{16}$ PAH and three 11-ring $C_{36}H_{16}$ PAH whose structures have not yet been determined. What we can say now, however, is that the $C_{28}H_{14}$ products in Figures 12 and 13 are likely key intermediates in the formation of these 10- and 11-ring PAH. The 10-ring $C_{34}H_{16}$ PAH can result from phenyl addition to $C_{28}H_{14}$ PAH (the type of reaction labelled “B” in Figure 13), followed by dehydrogenation. The 11-ring $C_{36}H_{16}$ PAH can result from methyl and benzyl addition to $C_{28}H_{14}$ PAH (the type of reaction sequence labelled “A” in Figure 13), followed by dehydrogenation. We thus see that the types of reaction mechanisms we have determined for the 2- to 8-ring product PAH in Figure 12 are also applicable to the formation of 10- and 11-ring PAH products of supercritical toluene pyrolysis—and by extension,

likely relevant to the formation of carbonaceous solids. Again, the HPLC/UV/MS instrument has played a key role in us being able to establish these findings.

Analysis of Stressed Fischer-Tropsch Synthetic Jet Fuel S-8 from UTRC

In our communications [55] with Dr. Tim Edwards at AFRL, we have learned that the Air Force is interested in a certain Fischer-Tropsch synthetic jet fuel S-8, for potential use in future high-speed aircraft. This fuel—which is composed of a mixture of C₁₀ to C₁₅ alkanes, both straight-chain (*n*-alkanes) as well as branched-chain (*iso*-alkanes)—has apparently formed higher-than-expected levels of carbonaceous solids in tests performed at UTRC. At Dr. Edwards' instigation, Dr. He Huang of UTRC sent us a set of samples from this fuel that had been “stressed” at supercritical conditions of 42 atm and temperatures of 590 to 710 °C. We have so far subjected three of these samples (635 °C, 674 °C, and 710 °C) to HPLC analysis—two of them to HPLC/UV only; the third to HPLC/UV/MS.

The chromatograms from our HPLC/UV/MS analyses—employing both the main and alternate solvent programs—of the 710-°C, 42-atm stressed S-8 fuel sample appear in Figures 16 and 17, respectively. The figures reveal that the stressed Fischer-Tropsch fuel sample contains 80 identified PAH of up to ten fused aromatic rings. Except for our own supercritical pyrolysis experiments with model alkane fuels, most of the PAH of > 6 rings in Figures 16 and 17 have never before been identified as products of alkane pyrolysis or combustion. As in the cases already discussed of the products of the model fuels 1-methylnaphthalene and toluene, most of the identifications of the Fischer-Tropsch synthetic jet fuel products have come from matching UV spectra with those of authentic reference standards or with those published for the reference standards. The structural determinations of three of the products in Figures 16 and 17—benz[*a*]anthanthrene, tribenzo[*cd,ghi,lm*]perylene, and dibenzo[*e,ghi*]naphtho[8,1,2-*klm*]perylene—have employed Annellation Theory, in conjunction with the UV spectra of appropriate

benzologues, since reference standards do not exist and UV spectra have never before been published for those compounds.

Another product of particular interest is benzo[*pqr*]dinaphtho[8,1,2-*bcd*:2',1',8'-*lmn*]perylene, the latest-eluting identified compound in Figure 17. The mass spectral and UV spectral evidence supporting the identification of this C₃₄H₁₆ ten-ring PAH is presented in Figure 18. Figure 18a establishes that the component eluting at 159 min in Figure 17 is of molecular mass 424 and molecular formula C₃₄H₁₆. Figure 18b shows the UV spectrum of the product component and that published [37] for the reference standard of benzo[*pqr*]dinaphtho[8,1,2-*bcd*:2',1',8'-*lmn*]perylene. Except for the spectral signal at 340-380 nm, which we have determined is due to an unidentified co-eluting product component, the two spectra in Figure 18b match well, confirming the identity of this product component as benzo[*pqr*]dinaphtho[8,1,2-*bcd*:2',1',8'-*lmn*]perylene. This is the first time that this C₃₄H₁₆ product has ever been identified as a product of an alkane fuel or as a product of a supercritical reaction environment. Although it is present in small amounts, its large molecular size and high length-to-breadth ratio may make it of particular significance in the formation of carbonaceous solids. Since this 10-ring PAH and several other high length-to-breadth-ratio products in Figures 16 and 17 do not appear in our supercritical pyrolysis products from our model aromatic fuels, we suspect that several of these products may be peculiar to the long-chain alkane nature of the Fischer-Tropsch synthetic jet fuel from which these products came. Because the UTRC tests have shown that this Fischer-Tropsch synthetic jet fuel is particularly prone to forming carbonaceous solids [55], supercritical pyrolysis experiments with representative alkanes are part of our proposed future work. Should this proposed work be funded, it is anticipated that the HPLC/UV/MS instrument will play a major role in product identification and reaction mechanism determination for the alkane fuels, just as it has already been shown to do in the cases of the model fuels examined so far.

Summary

Analysis of the products of supercritical 1-methylnaphthalene pyrolysis by high-pressure liquid chromatography with diode-array ultraviolet-visible absorbance detection and mass spectrometric detection (HPLC/UV/MS) has led to the identification of 37 individual 2- to 7-ring PAH—fifteen of which have never before been reported as products of 1-methylnaphthalene pyrolysis. The absence, among the reaction products, of single-ring aromatics and acetylene indicates that there is no aromatic ring rupture in this reaction environment, and the structures of each of the 5- to 7-ring PAH products reveal the intactness of the two 2-ring naphthalene units required in their construction. Proposed reaction pathways involving species plentiful in the reaction environment—1-naphthylmethyl radical, methyl radical, 1-methylnaphthalene, naphthalene, and 2-methylnaphthalene—account for the formation of the observed 5- to 7-ring PAH products. These reaction pathways, along with consideration of bond dissociation energies and relative abundances of reactant species, account for the extremely high product selectivity exhibited by the observed product PAH. The detection of six 8- and 9-ring PAH, each requiring construction from three naphthalene or methylnaphthalene units, provides evidence that the types of reaction mechanisms outlined here—for the combination of two naphthalene entities to form 5- to 7-ring PAH—are also likely to apply to the combination of three and more such entities in the formation of larger-ring-number PAH and eventually carbonaceous solids. HPLC/UV/MS analysis, in conjunction with Annellation Theory, has led to the identification of one of the 9-ring products, benzo[*cd*]phenanthro[1,2,3-*lm*]perylene, a $C_{34}H_{18}$ PAH that has never before been reported in the chemical literature.

HPLC/UV/MS analysis of the supercritical pyrolysis products of toluene, in conjunction with Annellation Theory, has led to the identification of six eight-ring benzenoid $C_{28}H_{14}$ PAH products

that have never before been identified as products of toluene pyrolysis or combustion. Determining, by HPLC/UV/MS, which particular PAH are produced and which are not has contributed to the elucidation of radical reaction mechanisms responsible for PAH formation and growth in the supercritical toluene pyrolysis environment. As in the case of 1-methylnaphthalene, there is no evidence of aromatic ring rupture in the supercritical toluene pyrolysis reaction environment, and PAH growth proceeds by combination of species plentiful in this environment—in this case: benzyl, phenyl, and methyl radicals, as well as toluene itself. These proposed reaction pathways account for the formation of the six observed $C_{28}H_{14}$ PAH products and explain why the other two benzenoid $C_{28}H_{14}$ PAH, determined by HPLC/UV/MS and Annellation Theory not to be present, are not formed. The detection, by HPLC/UV/MS, of seven 10-ring $C_{34}H_{16}$ and three 11-ring $C_{36}H_{16}$ PAH in the supercritical toluene pyrolysis products indicates that the benzyl-, phenyl-, and methyl-addition reactions responsible for the $C_{28}H_{14}$ PAH also take place with the $C_{28}H_{14}$ PAH, producing the higher-ring-number $C_{34}H_{16}$ and $C_{36}H_{16}$ products—and, by extension, carbonaceous solids.

HPLC/UV/MS analysis of the supercritical pyrolysis products in a stressed Fischer-Tropsch synthetic jet fuel sample provided by UTRC (at the instigation of Dr. Tim Edwards at AFRL) has led to the identification of 80 PAH of two to ten fused aromatic rings—many of which have never before been identified as products of alkane pyrolysis or combustion. Several of the identified PAH from the Fischer-Tropsch fuel do not appear in the products of our model aromatic fuels and have particularly high length-to-breadth ratios, a property that may be related to the long-chain alkane nature of the Fischer-Tropsch fuel. Because the UTRC tests have shown that this Fischer-Tropsch synthetic jet fuel is particularly prone to forming carbonaceous solids [55], supercritical pyrolysis experiments with representative alkanes are part of our proposed future work. Should this proposed work be funded, it is anticipated that the HPLC/UV/MS instrument will play a

major role in product identification and reaction mechanism determination for the alkane fuels, just as it has already been shown to do in the cases of the model fuels examined so far.

Publications and Presentations

Refereed Publications to which results from the HPLC/UV/MS instrument contributed

The first three of the refereed publications listed below pertain directly to the AFOSR-sponsored work on supercritical pyrolysis of model fuels. The fourth one pertains to a project on environmental atmospheric chemistry, for which the HPLC/UV/MS instrument was used to analyze oxygenated aromatics.

Somers, M. L., McClaine, J. W., and Wornat, M. J., "The Formation of Polycyclic Aromatic Hydrocarbons from the Supercritical Pyrolysis of 1-Methylnaphthalene," *Proceedings of the Combustion Institute 31*, in press, 2006.

McClaine, J. W., Zhang, X., and Wornat, M. J., "First Identification of Benzo[ghi]naphtho[8,1,2-bcd]perylene as a Product of Fuel Pyrolysis Using High-Performance Liquid Chromatography with Diode-Array Ultraviolet-Visible Absorbance Detection and Mass Spectrometry," *Journal of Chromatography A*, in press, 2006.

McClaine, J. W., and Wornat, M. J., "Reaction Mechanisms Governing the Formation of Polycyclic Aromatic Hydrocarbons in the Supercritical Pyrolysis of Toluene: C₂₈H₁₄ Isomers," submitted to *Journal of Physical Chemistry A*, 2006.

Chen, J., Valsaraj, K. T., Ehrenhauser, F. S., Wornat, M. J., "Uptake and Photooxidation of Gas-Phase Naphthalene on the Surface of Atmospheric Water Films," *Journal of Physical Chemistry A*, in press, 2006.

Conference presentations to which results from the HPLC/UV/MS instrument contributed

The first seven of the conference presentations listed below pertain directly to the AFOSR-sponsored work on supercritical pyrolysis of model fuels. The last two pertain to the analytical technique itself.

Somers, M. L., McClaine, J. W., and Wornat, M. J., "The Formation of Polycyclic Aromatic Hydrocarbons from the Supercritical Pyrolysis of 1-Methylnaphthalene," Thirty-First International Symposium on Combustion, Heidelberg, Germany, August, 2006.

Oña, J. O., and Wornat, M. J., "Perylene Benzologues: A Major Class of PAH Products from the Supercritical Pyrolysis of a Synthetic Jet Fuel," work-in-progress poster accepted for presentation at the Thirty-First International Symposium on Combustion, Heidelberg, Germany, August, 2006.

McClaine, J. W., Zhang, X., Oña, J. O., and Wornat, M. J., "Identification of

Benzo[ghi]naphtho[8,1,2-*bcd*]perylene: a New 8-Ring Benzenoid PAH Found as a Product of Supercritical Toluene Pyrolysis," work-in-progress poster accepted for presentation at the Thirty-First International Symposium on Combustion, Heidelberg, Germany, August, 2006.

Somers, M. L., Zhang, X., and Wornat, M. J., "The Detection and Identification of Polycyclic Aromatic Hydrocarbon Products from 1-Methylnaphthalene Pyrolysis," work-in-progress poster accepted for presentation at the Thirty-First International Symposium on Combustion, Heidelberg, Germany, August, 2006.

Bagley, S. P., Oña, J. O., and Wornat, M. J., "Formation of Polycyclic Aromatic Hydrocarbons from a Fischer-Tropsch Jet Fuel," work-in-progress poster accepted for presentation at the Thirty-First International Symposium on Combustion, Heidelberg, Germany, August, 2006.

Oña, J. O., and Wornat, M. J., "Identification of Perylene Benzologues in the Products of Supercritical Pyrolysis of a Fischer-Tropsch Synthetic Jet Fuel," submitted for presentation at the Fifty-Eighth Pittsburgh Conference on Analytical Chemistry and Applied Spectroscopy, Chicago, February-March, 2007.

Oña, J. O., and Wornat, M. J., "The Influence of Solvents on the UV Spectra of Polycyclic Aromatic Hydrocarbons: Applications in the Identification of Fuel Products by HPLC/UV/MS," submitted for presentation at the Fifty-Eighth Pittsburgh Conference on Analytical Chemistry and Applied Spectroscopy, Chicago, February-March, 2007.

Zhang, X., Somers, M. L., Robles, J. A., and Wornat, M. J., "Detection of Polycyclic Aromatic Hydrocarbons by Liquid Chromatography / Atmospheric Pressure Photoionization Mass Spectrometry," poster presentation at the Fifty-Fourth ASMS Conference on Mass Spectrometry and Allied Topics, Seattle, Washington, May, 2006.

Ehrenhauser, F. S., Alcanzare, R. J., Thomas, S., and Wornat, M. J., "Determination of Oxygenated Aromatics via HPLC Coupled to Atmospheric Pressure Photoionization Mass Spectrometry," work-in-progress poster accepted for presentation at the Thirty-First International Symposium on Combustion, Heidelberg, Germany, August, 2006.

References

1. T. Edwards, S. Zabarnick, *Industrial and Engineering Chemistry Research* 32 (1993) 3117-3122.
2. S. P. Heneghan, S. Zabarnick, D. R. Ballal, W. E. Harrison III, *Journal of Energy Resources Technology* 118 (1996) 170-179.
3. T. Dounghthip, J. S. Ervin, T. F. Williams, J. Bento, *Industrial and Engineering Chemistry Research* 41 (2002) 5856-5866.
4. T. Edwards, *Combustion Science and Technology* 178 (2006) 307-334.

5. H. Huang, D. R. Sobel, L. J. Spadaccini, 38th AIAA/ASME/SAE/ASEE Joint Propulsion Conference and Exhibit; Indianapolis, Indiana; July, 2002. Paper AIAA 2002-3871.
6. E. B. Ledesma, M. J. Wornat, P. G. Felton, J. A. Sivo, *Proceedings of the Combustion Institute* 30 (2005) 1371-1379.
7. M. J. Wornat, Final Technical Report for AFOSR Grant No. F49620-00-1-0298 (2003).
8. G. D. Davis, *An Experimental Study of Supercritical Methylcyclohexane Pyrolysis*, M.S.E. Thesis, Department of Mechanical and Aerospace Engineering, Princeton University, 1994.
9. J. F. Stewart, *Supercritical Pyrolysis of Endothermic Fuels*, Ph.D. Thesis, Department of Mechanical and Aerospace Engineering, Princeton University, 1999.
10. J. F. Stewart, K. Brezinsky, I. Glassman, *Combustion Science and Technology* 136 (1998) 373-390.
11. M. Somers, J. W. McClaine, M. J. Wornat, *Proceedings of the Combustion Institute* 31, in press (2006).
12. S. Darrah, "Jet Fuel Deoxygenation," AFWAL-TR-88-2081 (1988).
13. A. H. Cutler, M. J. Antal, M. Jones, *Industrial and Engineering Chemistry Research* 27 (1988) 691-697.
14. J. C. Y. Lee, *Simulations of Two-Dimensional Chemically Reactive Flows: Flow Past a Fuel Particle and Inside a Reactor Tube*, Ph.D. Thesis, Department of Mechanical and Aerospace Engineering, Princeton University, 1996.
15. R. N. Jones, *Journal of the American Chemical Society* 67 (1945) 2127-2150.
16. J. C. Fetzer, *Large ($C \geq 24$) Polycyclic Aromatic Hydrocarbons: Chemistry and Analysis*, Wiley-Interscience, New York, 2000, pp. 22, 70, 232.
17. E. V. Dose, G. Guiochon, *Analytical Chemistry* 61 (1989) 2571-2579.
18. X. Zhang, J. A. Robles, M. L. Somers, and M. J. Wornat, in preparation.
19. S. J. Bos, S. M. van Leeuwen, U. Karst, *Analytical and Bioanalytical Chemistry* 384 (2006) 85-99
20. M. Bernabei, R. Reda, R. Galiero, G. Bocchinfuso, *Journal of Chromatography A* 985 (2003) 197-203.
21. M. L. Somers, M. J. Wornat, to be submitted to *Polycyclic Aromatic Compounds*
22. L. Xiujin, *Sci. Sinica (Series B)* 29 (1986) 481-493

23. E. D. Bergmann, E. Fischer, Y. Hirshberg, D. Lavie, Y. Sprinzak, J. Szmuszkovicz, *Mémoires Présentés à la Société Chimique* 1953 (1953) 798-809.
24. S. A. Wise, R. M. Campbell, W. R. West, M. L. Lee, K. D. Bartle, *Chem. Geol.* 54 (1986) 339-357
25. R. N. Jones, *J. Am. Chem. Soc.* 67 (1945) 2021-2027
26. Y.-R. Luo, *Handbook of Bond Dissociation Energies in Organic Chemistry*, CRC Press, Boca Raton, FL, 2003, pp. 38, 39, 110.
27. R. T. Sanderson, *Chemical Bonds in Organic Compounds*, Sea and Sand, Scottsdale, AZ, 1976, Chapter 8.
28. M. Szwarc and A. Shaw, *Journal of the American Chemical Society* 73 (1951) 1379.
29. J. Yang, M. Lu, *Environmental Science and Technology* 39 (2005) 3077-3082
30. W. Schmidt, G. Grimmer, J. Jacob, G. Dettbarn, K.-W. Naujack, *Fresenius' Zeitschrift für Analytische Chemie* 326 (1987) 401-413.
31. J. V. Knop, W. R. Mueller, K. Szymanskik, and N. Trinajstić, *Computer Generation of Certain Classes of Molecules*, 1985, SKTH/Kemija u Industriji, Zegreb, 210 pages.
32. M. Zander and W. Franke, *Chemische Berichte* 94 (1961) 446-450.
33. E. J. Clar, *Journal of the Chemical Society [Abstracts]* 1949 (1949) 2013-2016
34. K. F. Lang, M. Zander, *Chemische Berichte* 98 (1965) 597-600
35. E. J. Clar, B. A. McAndrew, and J. F. Stephen, *Tetrahedron* 26 (1970) 5465-5478.
36. K. Maruyama, T. Otsuki, and K. Mitsui, *Journal of Organic Chemistry* 45 (1980) 1424-1428
37. E.J. Clar, *Polycyclic Hydrocarbons*, volume 2, Academic Press, New York, 1964
38. J. C. Fetzer, Chapter 18 in *Polyuclear Aromatic Hydrocarbons*, ed. by L. Ebert. *Advances in Chemistry* 217. American Chemical Society: Washington D. C. (1988) 309-331.
39. J. C. Fetzer and W. R. Biggs, *Journal of Chromatography* 322 (1985) 275-286.
40. J. C. Fetzer and W. Schmidt, *Spectrochimica Acta A* 45A (1989) 503-505.
41. E. J. Clar, J. F. Guye-Vuilleme, and J. F. Stephen, *Tetrahedron* 20 (1964) 2107-2117.
42. S. A. Wise, L. C. Sander, and W. E. May, *Journal of Chromatography* 642 (1993) 329-349.
43. L. C. Sander, M. Pursch, and S. A. Wise, *Analytical Chemistry* 71 (1999) 4821-4830.

44. S. A. Wise and L. C. Sander, *Journal of High Resolution Chromatography & Chromatography Communications* 8 (1985) 248-255.
45. T. Umemoto, T. Kawashima, Y. Sakata, and S. Misumi, *Tetrahedron Letters* 12 (1975) 1005-1006.
46. J. W. McClaine, X. Zhang, M. J. Wornat, *Journal of Chromatography A*, in press (2006).
47. J. C. Fetzer, W. R. Biggs, and K. Jinno, *Chromatographia* 21 (1986) 439-442.
48. J. C. Fetzer and J. R. Kershaw *Fuel* 74 (1995) 1533-1536.
49. A. L. Lafleur, K. Taghizadeh, J. B. Howard, J. F. Anacleto, M. A. Quilliam *J. Am. Soc. Mass Spectrom.* 7 (1996) 276-286.
50. J. C. Fetzer and W. R. Biggs, *Polycyclic Aromatic Compounds* 5 (1994) 193-198
51. L. Ojakaar, Ph. D. Thesis. Virginia Polytechnic University, 1964.
52. F. A. Vingiello, L. Ojakaar, *Tetrahedron* 22 (1966) 847-860.
53. J. W. McClaine, J. O. Oña, and M. J. Wornat, in preparation.
54. J. W. McClaine, M. J. Wornat, submitted to *Journal of Physical Chemistry A*.
55. T. Edwards, personal communication, AFRL, Wright-Patterson, Ohio, October, 2005.

Table 1. Products of Supercritical 1-Methylnaphthalene Pyrolysis at 585°C, 110 atm, 140 sec.

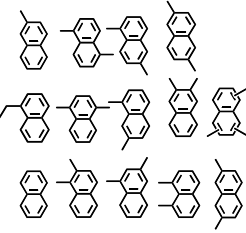
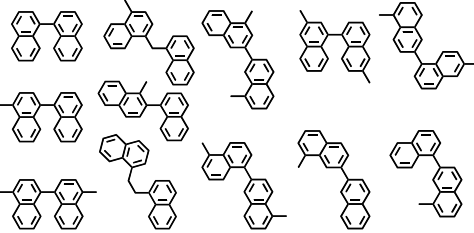
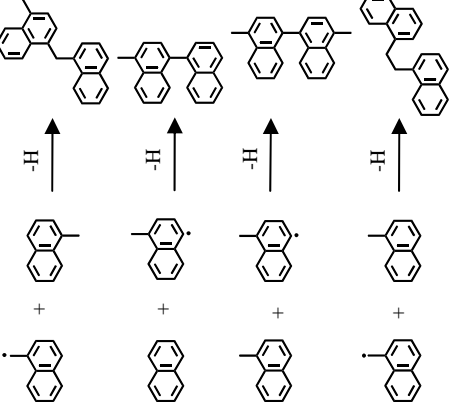
Products	Reactions Responsible for Product Formation	Findings
	<p>Displacement of methyl by hydrogen, e.g.</p> $\text{1-methylnaphthalene} + \text{H}\cdot \longrightarrow \text{naphthalene} + \cdot\text{CH}_3$ <p>Displacement of hydrogen by methyl, e.g.</p> $\text{1-methylnaphthalene} + \cdot\text{CH}_3 \longrightarrow \text{1,2-dimethylnaphthalene} + \text{H}\cdot$	<p>Under the supercritical pyrolysis reaction conditions, it is possible to break the following bonds:</p> <ul style="list-style-type: none"> methyl C-H BDE 85.1 kcal/mol methyl-aryl C-C BDE 103.8 kcal/mol aryl C-H BDE 112.2 kcal/mol <p>It is not possible to break the aromatic C-C bond: aromatic C-C BDE 122.3 kcal/mol</p>
 <p>(Some examples of more than 30 configurations of bi-naphthyls)</p>	<p>Displacement of hydrogen or methyl by naphthyl/methyl, methyl/naphthyl, or naphthyl</p> 	<p>The two 2-ring naphthalene units stay intact as the methyl and hydrogen displacements take place to form the bi-naphthyls.</p>

Table 1 (continued). Products of Supercritical 1-Methylnaphthalene Pyrolysis at 585°C, 110 atm, 140 sec.

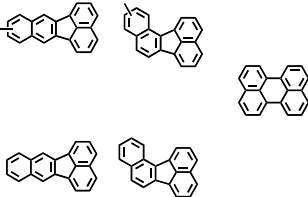
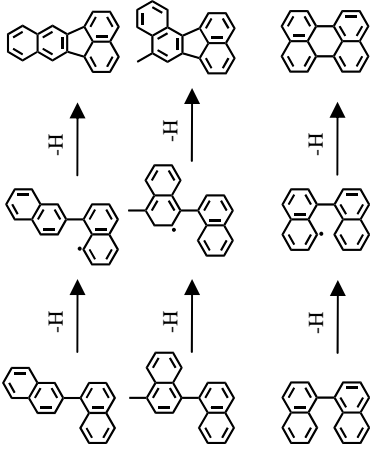
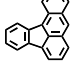
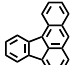
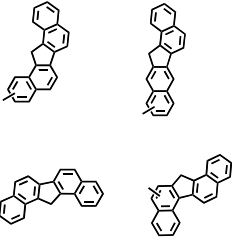
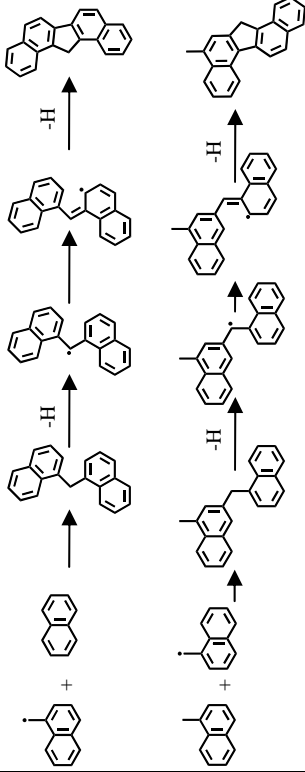
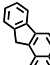
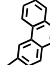
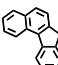
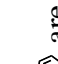
Products	Reactions Responsible for Product Formation	Findings
<p>Class 3: Five-Ring $C_{20}H_{12}$ PAH and their Methyl Derivatives (blue structures in Figure 2)</p> 	<p>Cyclodehydrogenation of bi-naphthyls and methylated bi-naphthyls, e.g.</p> 	<p>The intactness of the original two 2-ring naphthalene units is preserved in the $C_{20}H_{12}$ five-ring PAH products.</p> <p>Isomers of the Class 3 products such as  and  are not produced since their formation does not require the addition of two 2-ring naphthalene units but rather a 1-ring and a 3-ring structure, which are not present in the supercritical 1-methylnaphthalene pyrolysis environment.</p>
<p>Class 4: Five-Ring $C_{21}H_{14}$ Dibenzofluorenes and their Methyl Derivatives (green structures in Figure 2)</p> 	<p>1-naphthylmethyl radical displacement of an aryl H of either naphthalene or a methylnaphthalene, followed by dehydrogenation, e.g.</p> 	<p>The intactness of the original two 2-ring naphthalene units is preserved in the $C_{21}H_{14}$ five-ring PAH products.</p> <p>Isomers of the Class 4 products such as  and  are not produced since their formation does not require the addition of two 2-ring naphthalene units but rather a 1-ring and a 3-ring structure, which are not present in the supercritical 1-methylnaphthalene pyrolysis environment.</p> <p>Isomers of the Class 4 products such as  and  are not observed here either since their formation requires a 2-naphthylmethyl adding to a "2" position of naphthalene, rather than the more plentiful 1-naphthylmethyl and "1" position.</p>

Table 1 (continued). Products of Supercritical 1-Methylnaphthalene Pyrolysis at 585°C, 110 atm, 140 sec.

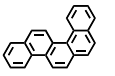
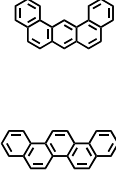
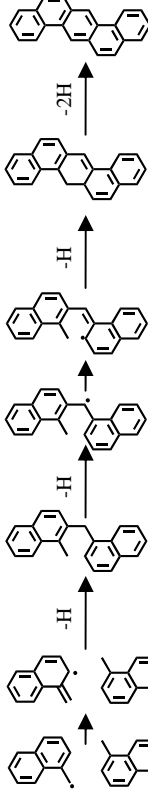
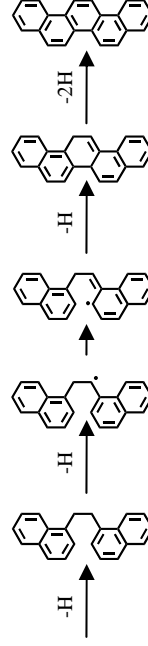
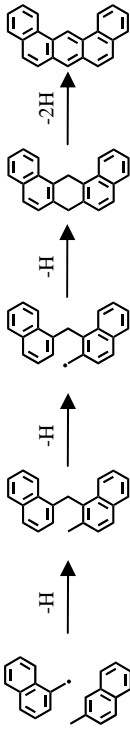
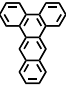
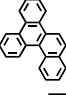
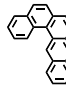
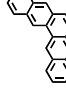
Products	Reactions Responsible for Product Formation	Findings
<p>Class 5: Five-Ring $C_{22}H_{14}$ PAH (red structures in Figure 2)</p>  	<p>Addition of 1-naphthylmethyl radical (or its resonance structure) to either 1-methylnaphthalene or 2-methylnaphthalene, followed by dehydrogenation, e.g.</p>   	<p>The intactness of the original two 2-ring naphthalene units is preserved in the $C_{22}H_{14}$ five-ring PAH products.</p> <p>Isomers of the Class 5 products such as  and  are not produced since their formation does not require the addition of two 2-ring naphthalene units but rather one 2-ring naphthalene unit and two 1-ring structures, the latter of which are not present in the supercritical 1-methylnaphthalene pyrolysis environment.</p> <p>Isomers of the Class 5 products such as  and  are not observed since their formation requires addition of 2-naphthylmethyl radical to 2-methylnaphthalene, which are much less plentiful than the "1-" counterparts in a 1-methylnaphthalene reaction environment.</p>

Table 1 (continued). Products of Supercritical 1-Methylnaphthalene Pyrolysis at 585°C, 110 atm, 140 sec.

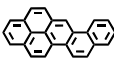
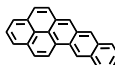
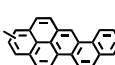
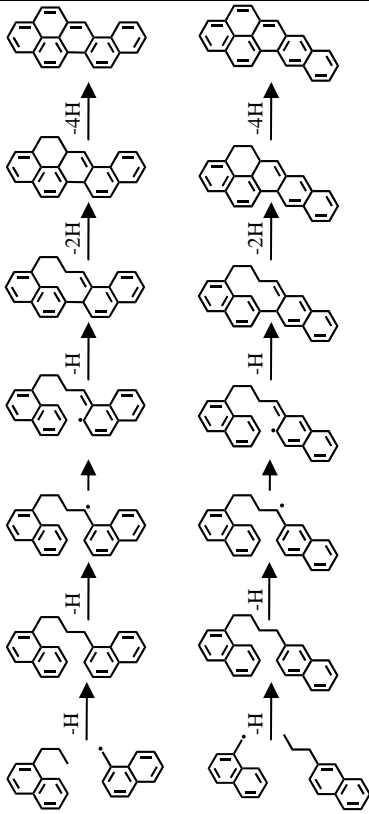
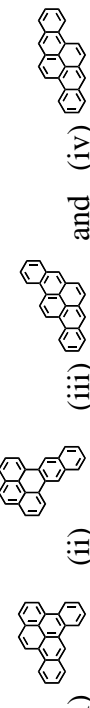
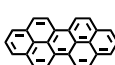
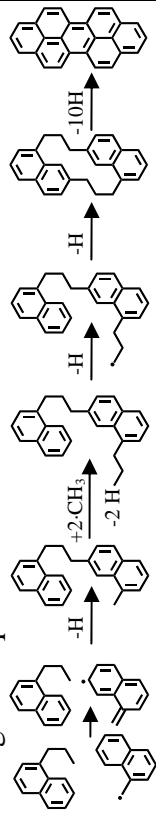
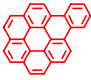


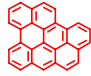
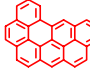
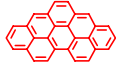

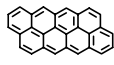
Products	Reactions Responsible for Product Formation	Findings
<p>Class 6: Six- and Seven-Ring PAH</p> <p>(a) $C_{24}H_{14}$ PAH and $CH_3-C_{24}H_{14}$ PAH</p>  <p>Naphtho[2,1-a]pyrene</p>  <p>Naphtho[2,3-a]pyrene</p>  <p>Methylated naphtho[2,1-a]pyrene</p>	<p>(a) Methyl addition twice to a methylnaphthalene to form a propylnaphthalene, then addition of 1-naphthylmethyl and dehydrogenation</p> 	<p>(a) $C_{24}H_{14}$ isomers such as</p>  <p>(i) (ii) (iii) and (iv)</p> <p>are not formed since: (i) their structures do not preserve the intactness of two 2-ring naphthalene units, (ii) their formation would require at least one of the naphthalene units to have been alkylated in the “2” position, (iii) their formation would require the methyl additions to occur at aryl rather than alkyl positions (the latter being favored for BDE reasons), or (iv) their formation would require the reaction of 1-naphthylethyl with 1-ethylnaphthalene, an unlikely scenario in a reaction environment dominated by 1-methylnaphthalene.</p>
<p>(b) $C_{26}H_{14}$</p>  <p>Dibenzo[cd,lm]perylene</p>	<p>(b) Same as (a) but with two additional methyl additions along the sequence</p> 	<p>(b) Just as in the cases of the 5- and 6-ring products, high product selectivity is observed for the 7-ring PAH, as dibenzo[cd,lm]perylene is the only $C_{26}H_{14}$ product detected.</p>

Table 2. C₂₈H₁₄ Benzenoid PAH

Benzo[<i>a</i>]coronene		Established as products of supercritical toluene pyrolysis by matching UV spectra with those of authentic reference standards
Benzo[<i>pqr</i>]naphtho[8,1,2- <i>bcd</i>]perylene		
Phenanthro[5,4,3,2- <i>efghi</i>]perylene		Established as products of supercritical toluene pyrolysis by confirming C ₂₈ H ₁₄ formulas from mass spectra and matching UV spectra with those published for the reference standards
Benzo[<i>cd</i>]naphtho[8,1,2,3- <i>fghi</i>]perylene		
Benzo[<i>ghi</i>]naphtho[8,1,2- <i>bcd</i>]perylene		Deduced as products of supercritical toluene pyrolysis from HPLC elution times, mass spectra, UV spectra, and Annellation Theory
Tribenzo[<i>cd,ghi,lm</i>]perylene		
Bisanthene		Determined not to be a product of supercritical toluene pyrolysis, from the published UV spectrum of the reference standard
Naphthaceno[3,4,5,6,7- <i>defghij</i>]naphthacene		Deduced not to be a product of supercritical toluene pyrolysis, from UV spectral characteristics predicted from Annellation Theory

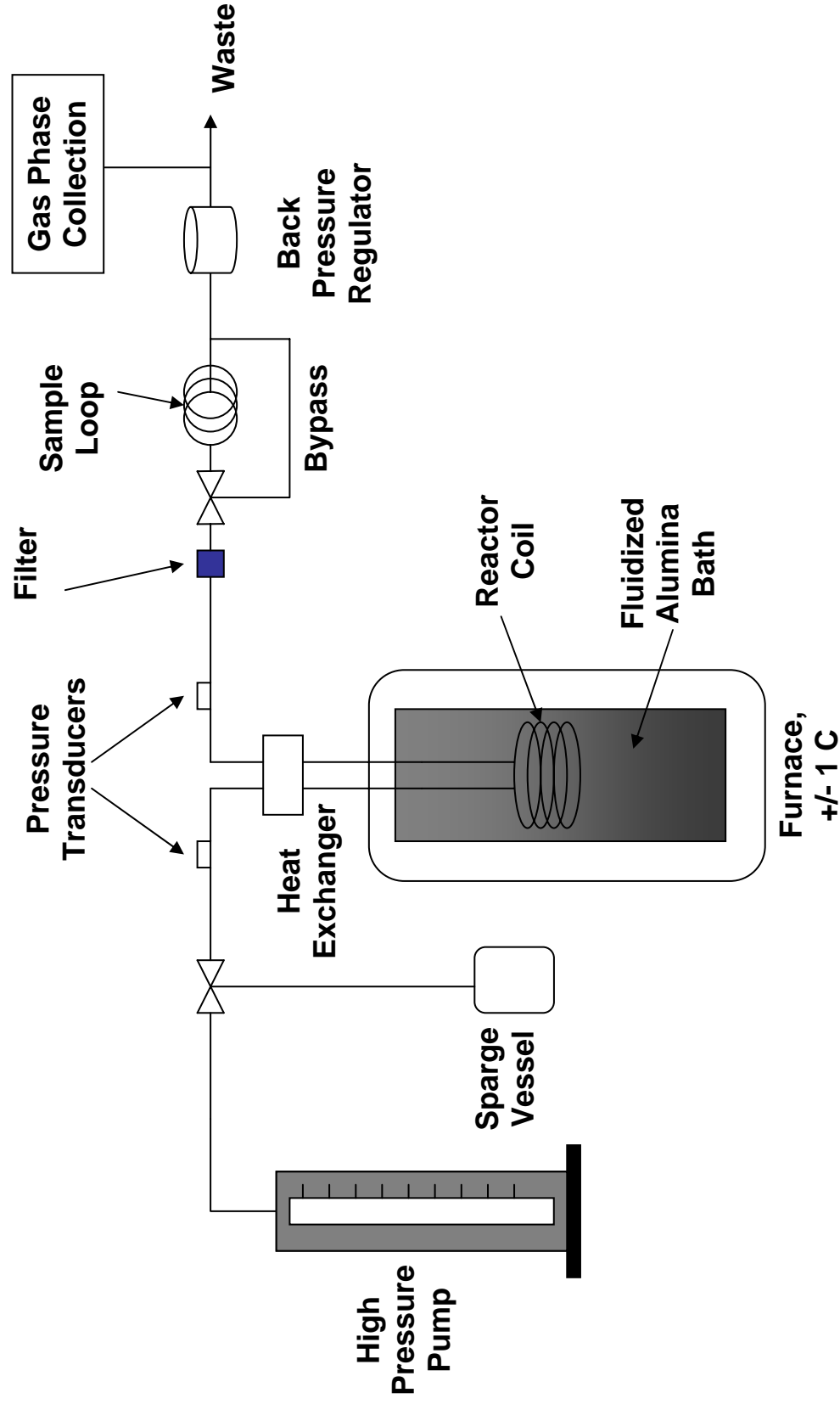


Figure 1. Supercritical fuels pyrolysis reactor system. Adapted from Stewart [9].

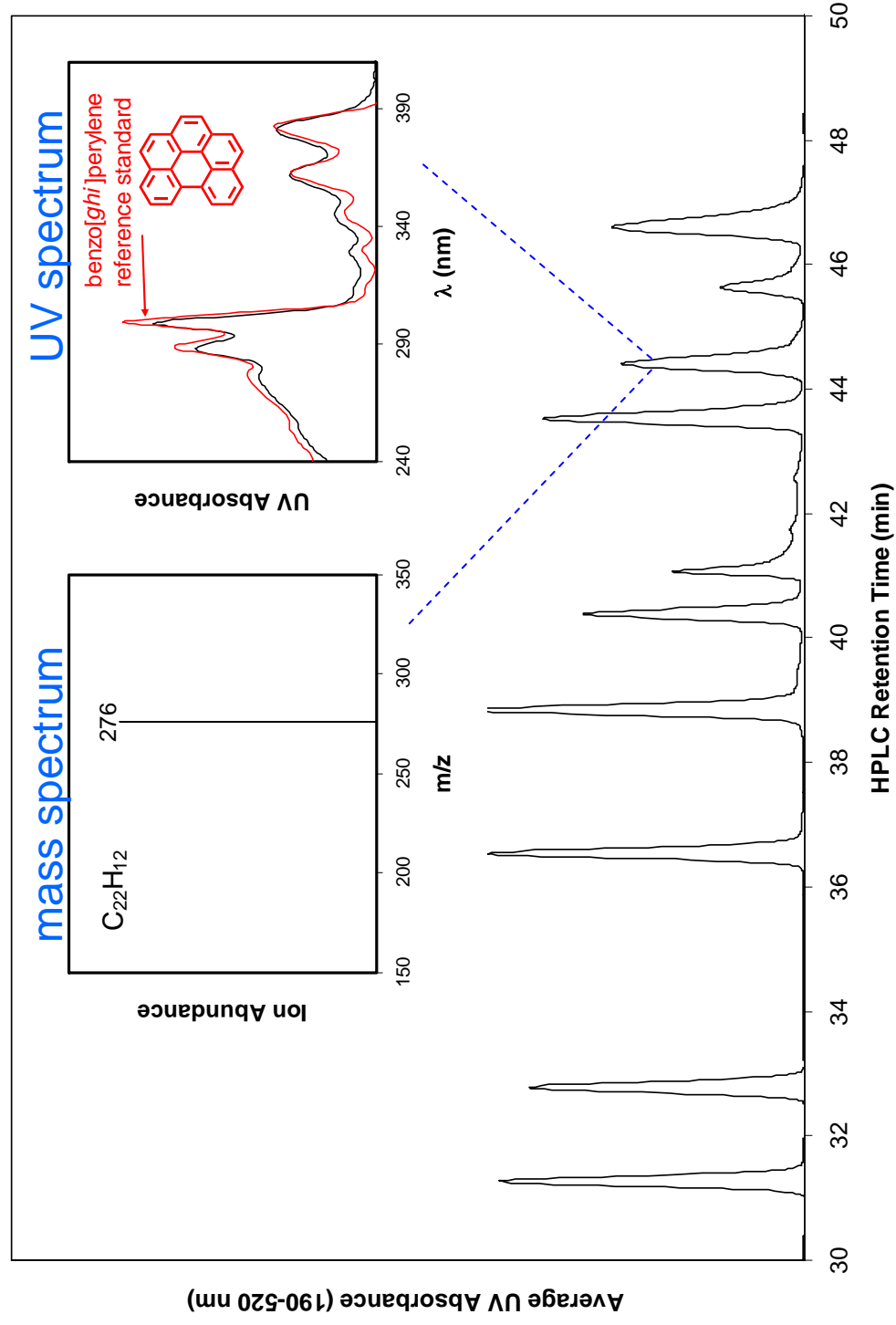


Figure 2. Illustration of the HPLC/UV/MS analysis technique. The left inset is the mass spectrum of the component eluting at 44.4 min in the HPLC chromatogram. The black curve in the right inset is the UV spectrum of this same component; the red curve in the right inset is the UV spectrum of a reference standard of benzo[ghi]perylene.

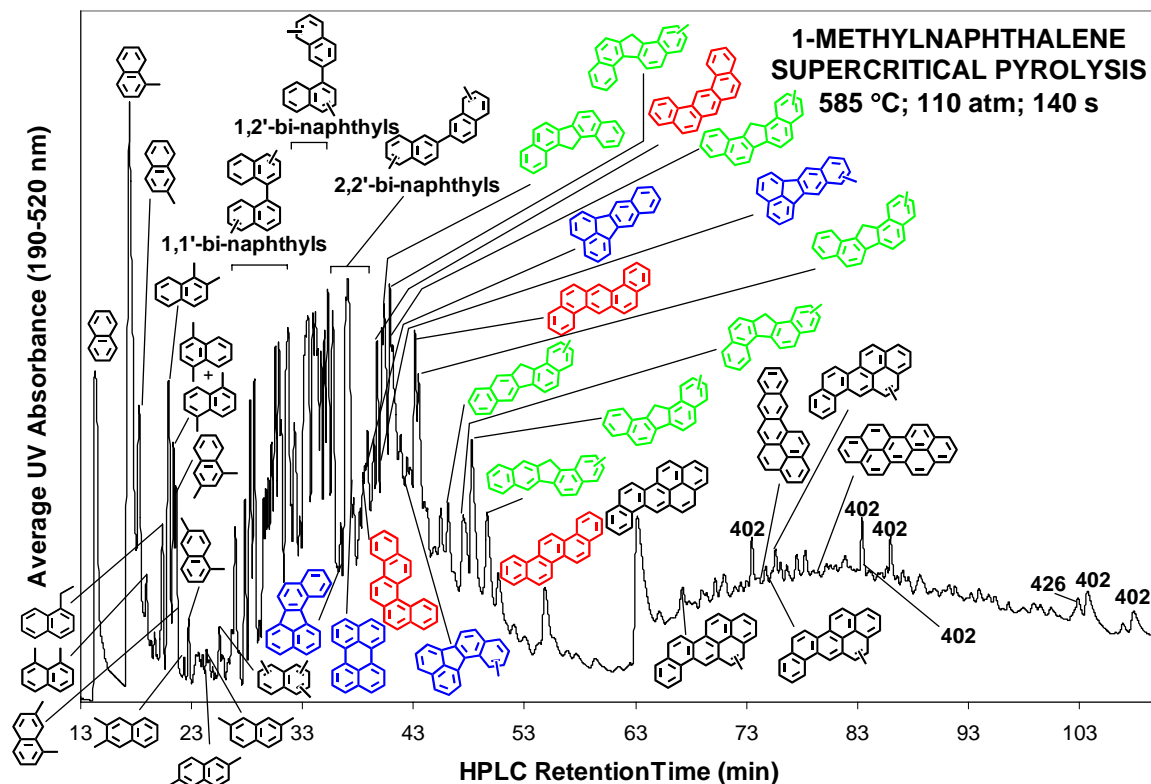


Figure 3. HPLC chromatogram of products of 1-methylnaphthalene pyrolyzed at 585 °C, 110 atm, and 140 sec. The rise in baseline at 63 minutes corresponds to a change in mobile-phase composition to UV-absorbing dichloromethane. Identified products of Classes 1 and 2 (in order of elution) are: naphthalene; 1-methylnaphthalene; 2-methylnaphthalene; 1,8-dimethylnaphthalene; 1-ethylnaphthalene; 1,2-dimethylnaphthalene; 1,4- and 1,5-dimethylnaphthalene; 1,3- and 1,7-dimethylnaphthalene; 2,3-dimethylnaphthalene; 1,6-dimethylnaphthalene; 2,6-dimethylnaphthalene; 2,7-dimethylnaphthalene; trimethylnaphthalene; 1,1'-bi-naphthyls; 1,2'-bi-naphthyls; and 2,2'-bi-naphthyls. Identified products of ≥ 5 rings, by class (in order of elution, from left to right) are: Class 3 (blue): benzo[*j*]fluoranthene; perylene; benzo[*k*]fluoranthene; methylbenzo[*k*]fluoranthene; methylbenzo[*j*]fluoranthene. Class 4 (green): dibenzo[*a,i*]fluorene; methyldibenzo[*a,g*]fluorene; methyldibenzo[*a,i*]fluorene; methyldibenzo[*a,i*]fluorene; methyldibenzo[*a,h*]fluorene; methyldibenzo[*a,g*]fluorene; methyldibenzo[*a,i*]fluorene; methyldibenzo[*a,h*]fluorene. Class 5 (red): benzo[*c*]chrysene; dibenz[*a,j*]anthracene; dibenz[*a,h*]anthracene; picene. Class 6 (black): naphtho[2,1-*a*]pyrene; methylnaphtho[2,1-*a*]pyrene; naphtho[2,3-*a*]pyrene; methylnaphtho[2,1-*a*]pyrene; methylnaphtho[2,1-*a*]pyrene; dibenzo[*cd,lm*]perylene. Numbers “402” and “426” signify molecular masses of PAH whose exact structures have not yet been determined.

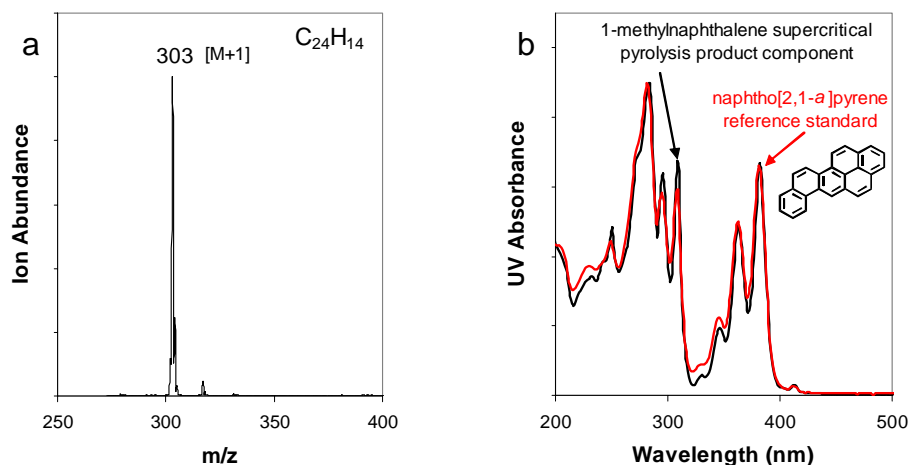


Figure 4. The (a) mass spectrum and (b) UV spectrum of the supercritical 1-methylnaphthalene pyrolysis product component eluting at 63.3 min in Figure 3. Due to proton transfer from the solvent methanol, the primary ion in the mass spectrum is at $M+1$, so $M = 302$. The UV spectrum of a reference standard of naphtho[2,1-*a*]pyrene is included in (b) to confirm the product component's identity as naphtho[2,1-*a*]pyrene.

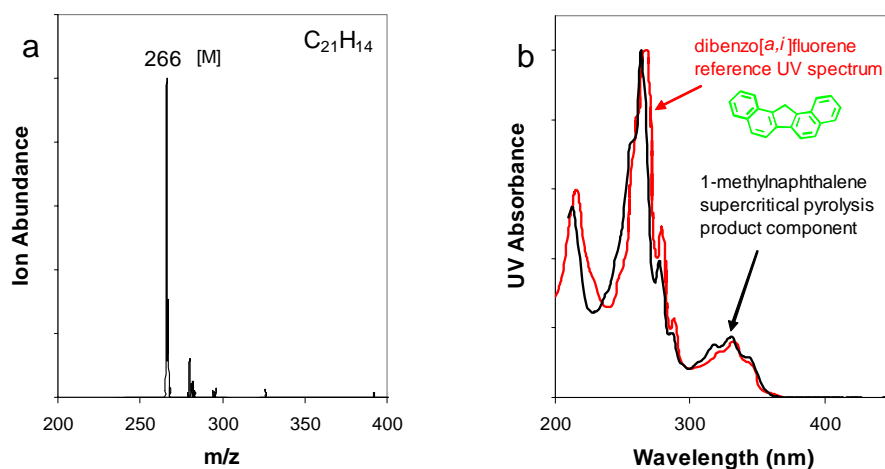


Figure 5. The (a) mass spectrum and (b) UV spectrum of the supercritical 1-methylnaphthalene pyrolysis product component eluting at 40.4 min in Figure 3. Since the solvent is acetonitrile, no proton transfer from the solvent occurs, and the primary ion in the mass spectrum is at M , so $M = 266$. The published [22] UV spectrum of dibenzo[*a,i*]fluorene is included in (b) to confirm the product component's identity as dibenzo[*a,i*]fluorene.

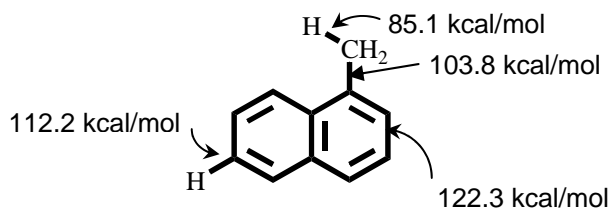


Figure 6. 1-Methylnaphthalene bond dissociation energies [26,27]

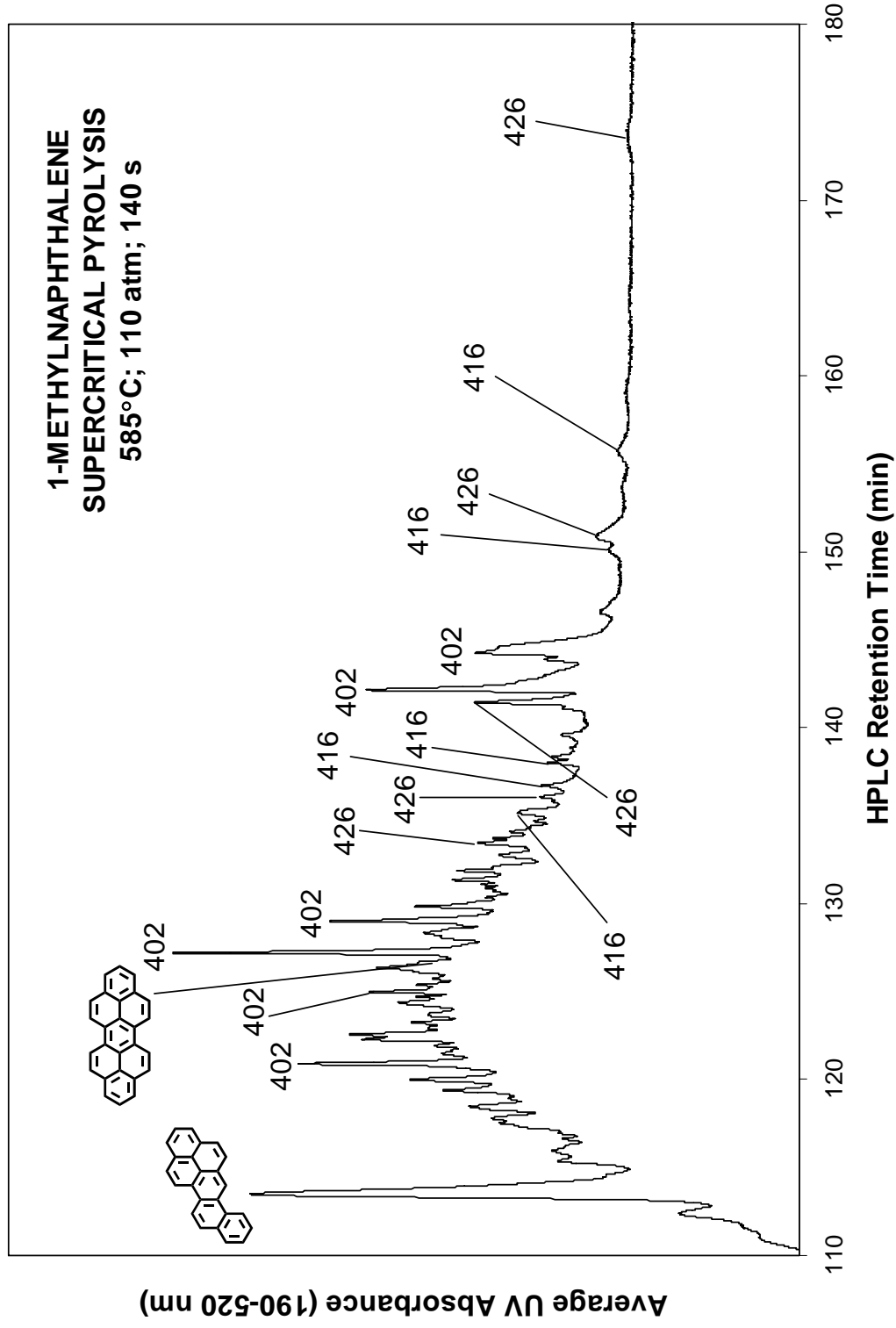


Figure 7. Final portion of the HPLC chromatogram (from a methanol/dichloromethane solvent program) of the products of 1-methylnaphthalene pyrolyzed at 585°C, 110 atm, and 140 sec. Numbers “402,” “416,” and “426” signify molecular masses of 8- and 9-ring PAH product components.

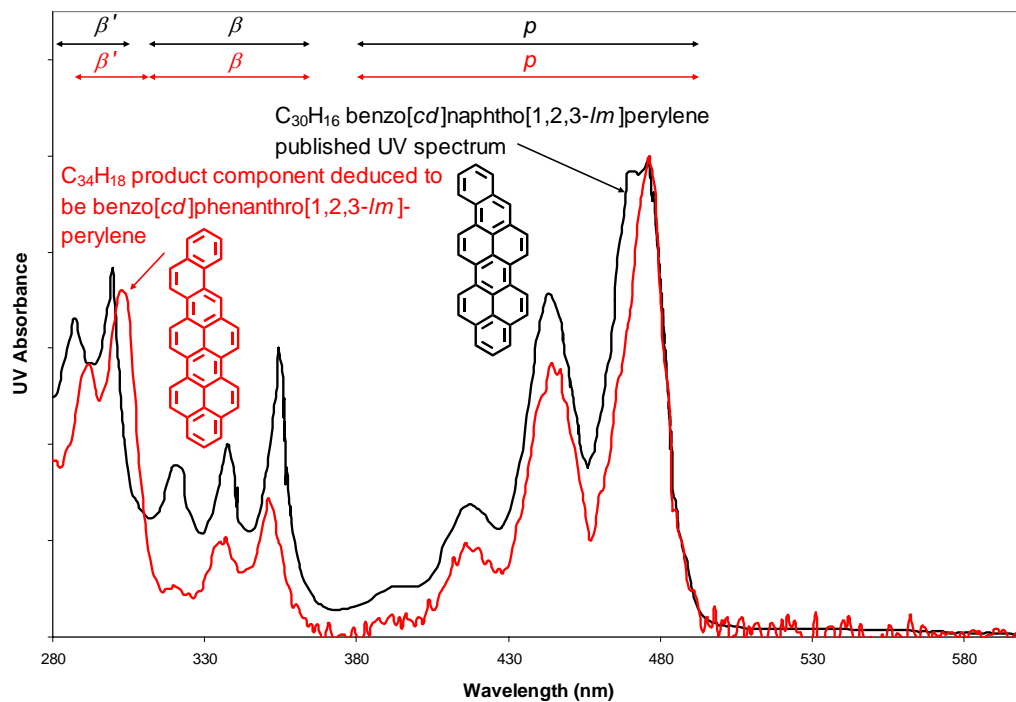


Figure 8. UV spectrum (in red) of the 1-methylnaphthalene product component eluting at 174 min in Figure 7, along with the published [16] UV spectrum (in black) of benzo[cd]naphtho[1,2,3-*lm*]perylene.

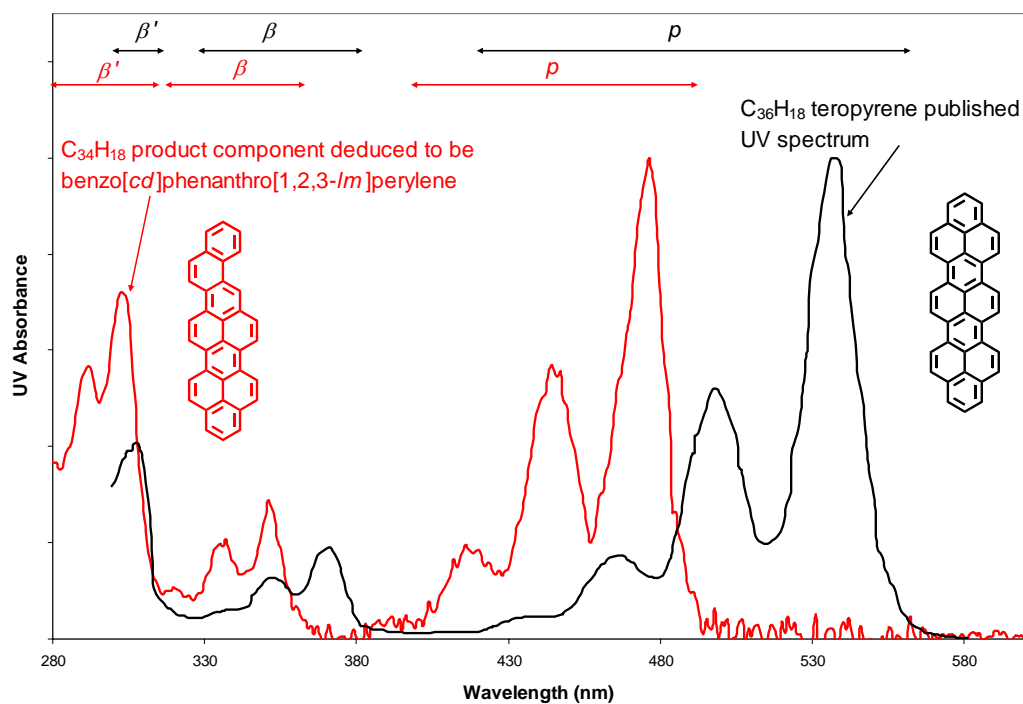


Figure 9. UV spectrum (in red) of the 1-methylnaphthalene product component eluting at 174 min in Figure 7, along with the published [45] UV spectrum (in black) of teropyrene.

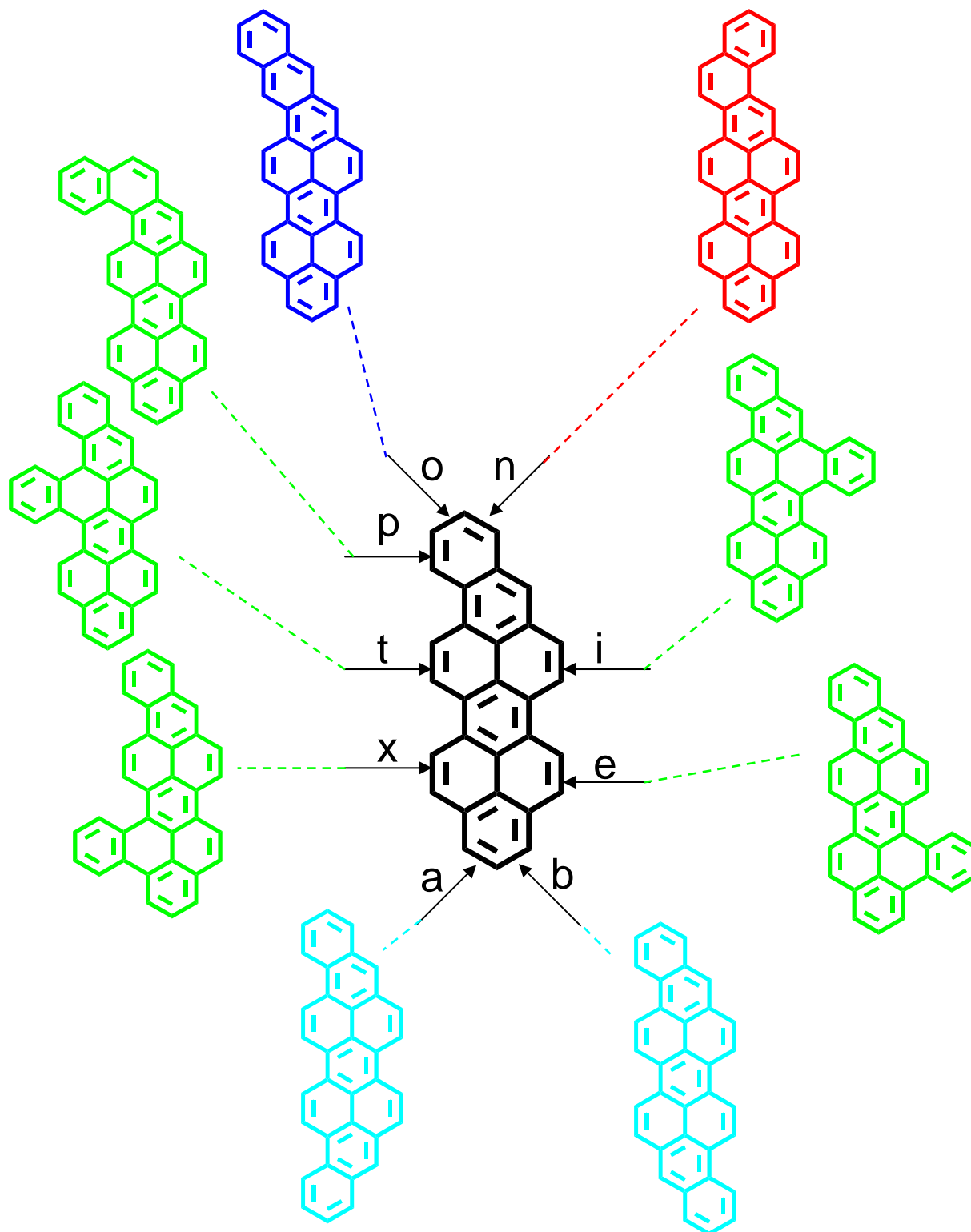


Figure 10. Benzo[*cd*]naphtho[1,2,3-*lm*]perylene and the 9 possible benzenoid C₃₄H₁₈ that can result from ring fusion to benzo[*cd*]naphtho[1,2,3-*lm*]perylene. Benzo[*cd*]phenanthro[1,2,3-*lm*]perylene, shown in red, is deduced to be the 1-methylnaphthalene product component eluting at 174 min in Figure 7.

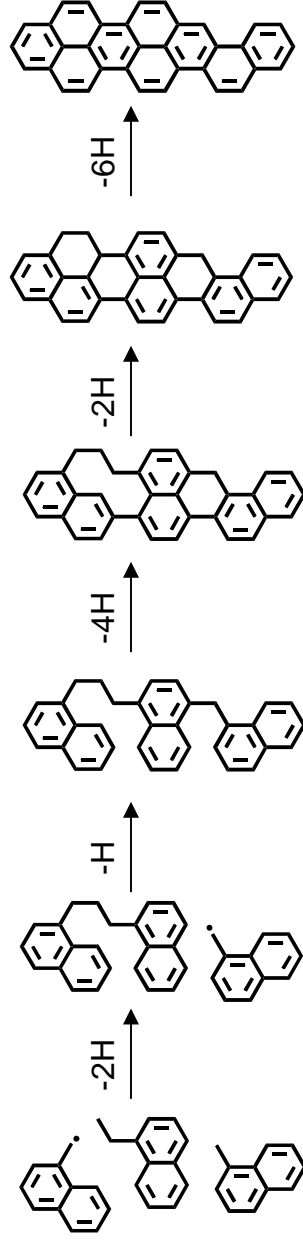


Figure 11. Proposed reaction mechanism for benzo[cd]phenanthro[1,2,3-*m*]perylene.

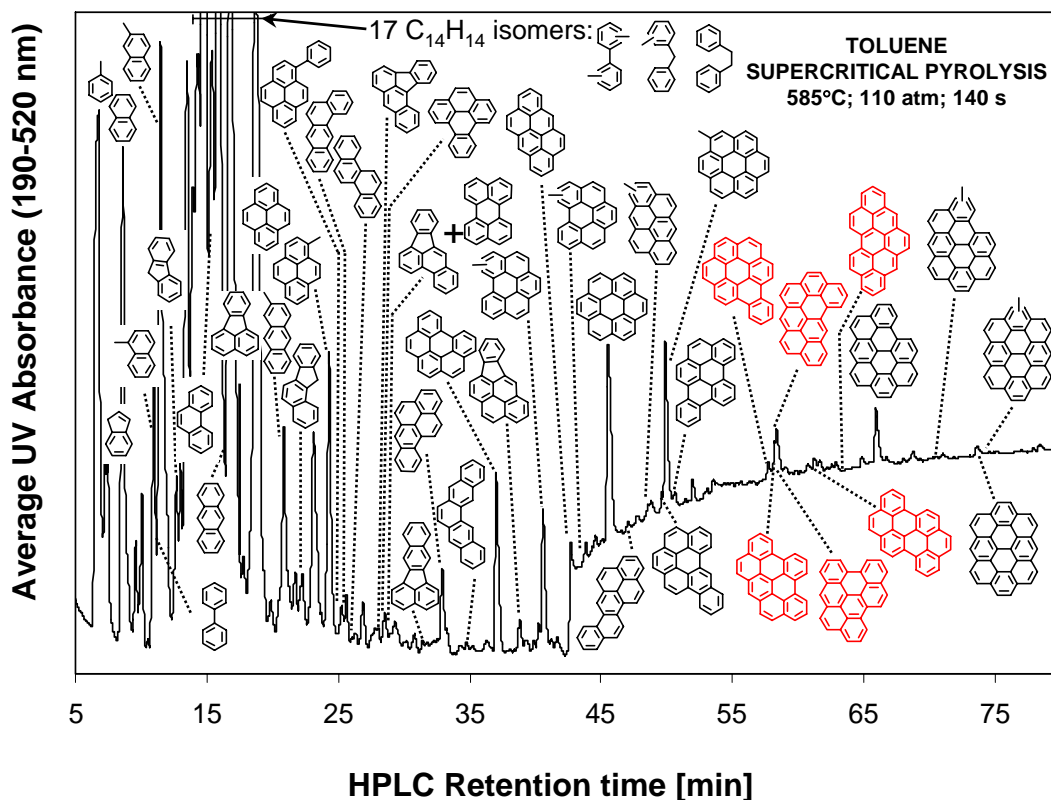


Figure 12. HPLC chromatogram of products of supercritical toluene pyrolysis at 535°C, 100 atm, and 140 s residence time. The rise in the baseline at ~43 min is due to a change in the mobile phase to the UV-absorbing dichloromethane. Identified components, in order of elution, from left to right, are: toluene, indene, naphthalene, 1-methylnaphthalene, bi-phenyl, 2-methylnaphthalene, fluorene, phenanthrene, anthracene, fluoranthene, pyrene, 2-methylanthracene, benzo[*a*]fluorene, 1-methylpyrene, 1-phenylpyrene, benz[*a*]anthracene, chrysene, benzo[*a*]fluoranthene, benzo[*e*]pyrene, benzo[*b*]fluoranthene co-eluting with perylene, benzo[*k*]fluoranthene, benzo[*a*]pyrene, pentaphene, benzo[*ghi*]perylene, indeno[1,2,3-*cd*]pyrene, methylated benzo[*ghi*]perylene, anthanthrene, methylated benzo[*ghi*]perylene, coronene, naphtho[2,1-*a*]pyrene, methylated anthanthrene, dibenzo[*b,ghi*]perylene, 1-methylcoronene, dibenzo[*e,ghi*]perylene, benzo[*a*]coronene, phenanthro[5,4,3,2-*efghi*]perylene, benzo[*cd*]naphtho[8,1,2,3-*fghi*]perylene, benzo[*ghi*]naphtho[8,1,2-*bcd*]perylene, benzo[*pqr*]naphtho[8,1,2-*bcd*]perylene, tribenzo[*cd,ghi,lm*]perylene, naphtho[8,1,2-*abc*]coronene, methylated naphtho[8,1,2-*abc*]coronene, ovalene, and methylated ovalene. Red structures correspond to C₂₈H₁₄ PAH.

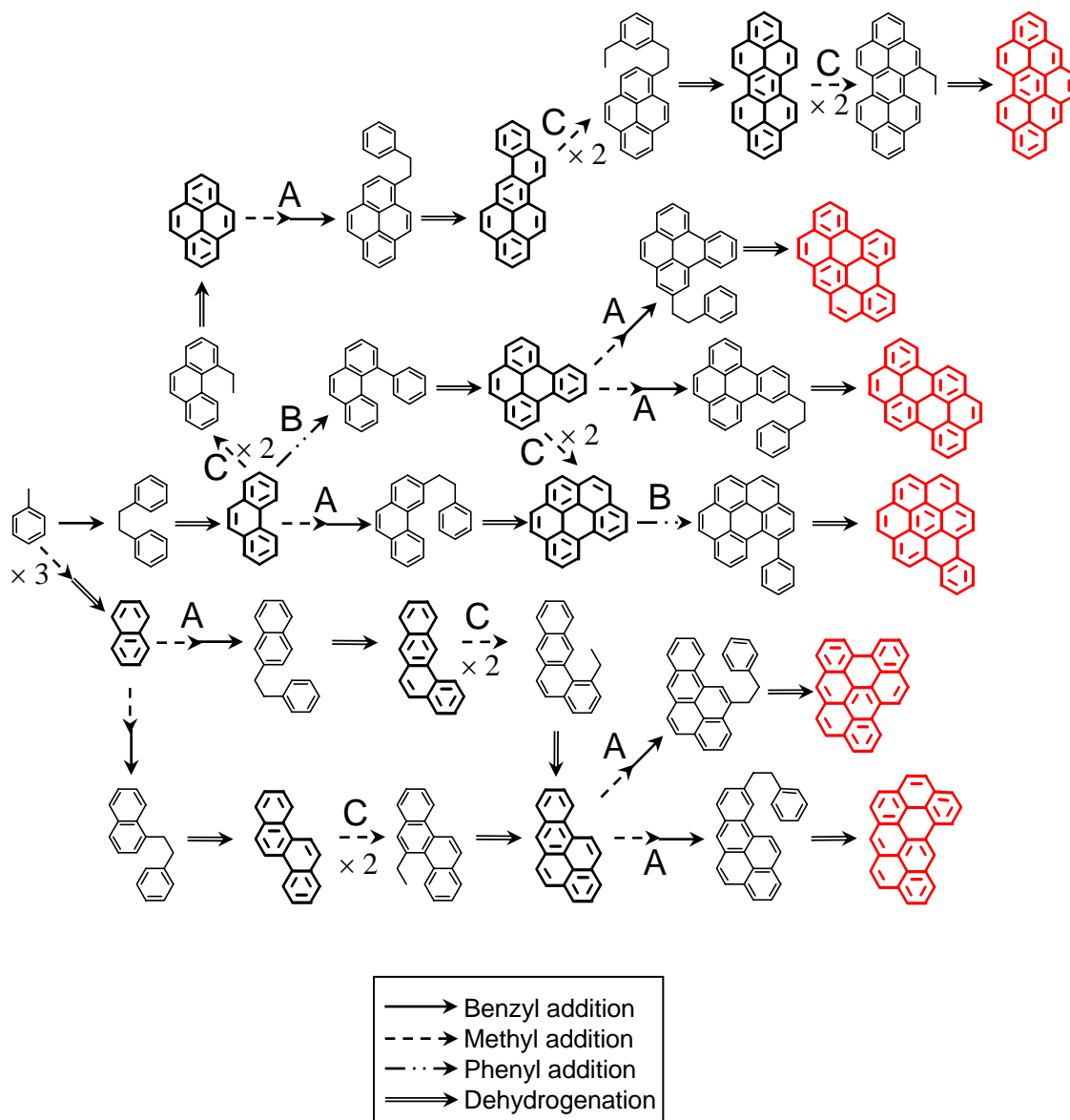


Figure 13. Reaction mechanisms to describe the formation of the six $C_{28}H_{14}$ PAH (shown in red) produced by supercritical toluene pyrolysis. In order from top to bottom, the $C_{28}H_{14}$ PAH are: tribenzo[*cd,ghi,lm*]perylene, phenanthro[5,4,3,2-*efghi*]perylene, benzo[*pqr*]naphtho[8,1,2-*bcd*]perylene, benzo[*a*]coronene, benzo[*cd*]naphtho[8,1,2,3-*fghi*]perylene, and benzo[*ghi*]naphtho[8,1,2-*bcd*]perylene. The formation of large PAH is shown through addition of methyl (dashed arrow), benzyl (solid arrow), and phenyl (dashed-dotted arrow) radicals. Dehydrogenation is shown as the double-lined arrow. In general, the three types of reactions are: (A) addition of methyl followed by benzyl, (B) addition of phenyl, and (C) addition of two methyls. Structures shown in bold print are PAH that have been identified, by their UV spectra, as products of the supercritical pyrolysis of toluene.

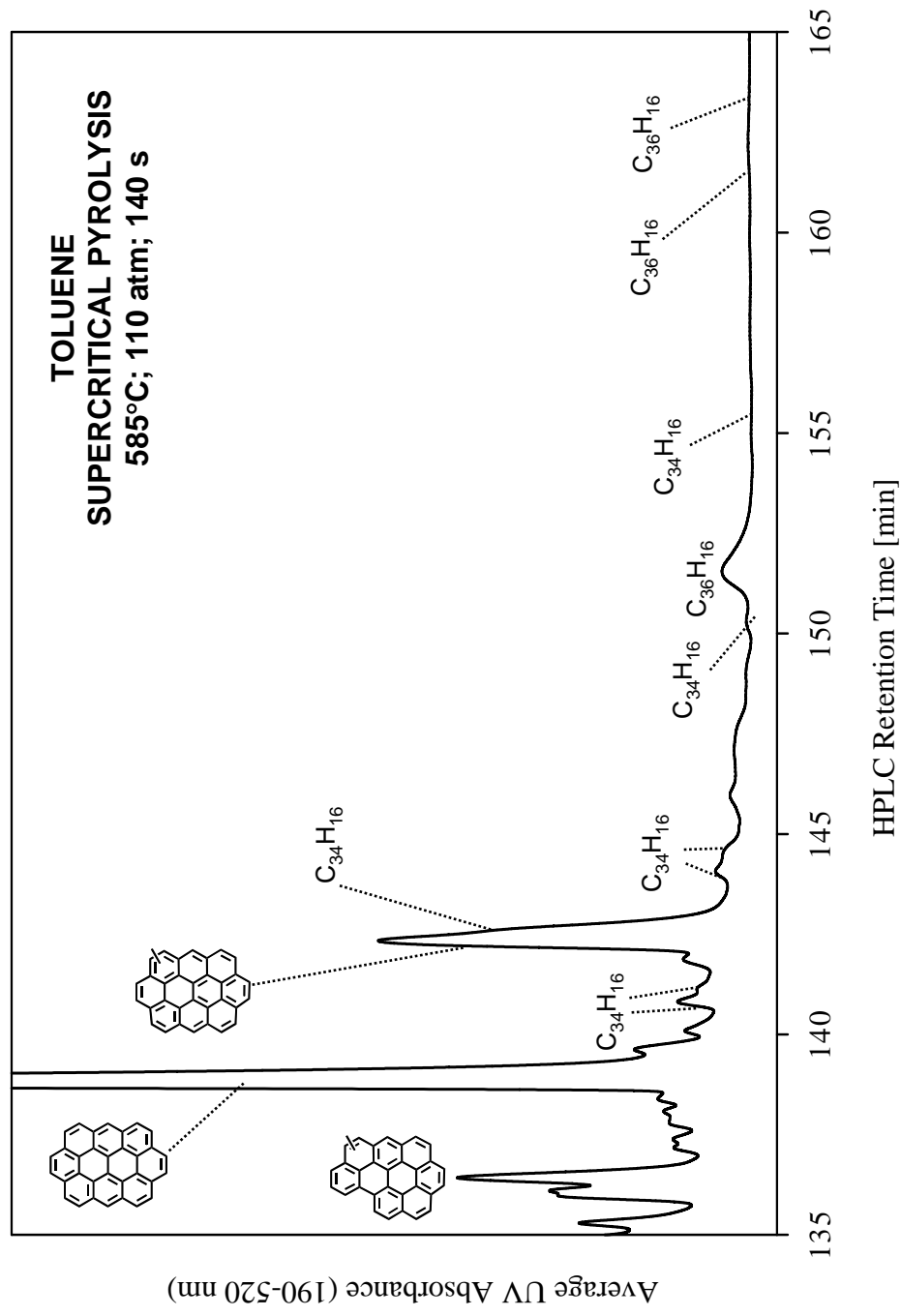


Figure 15. Final portion of the HPLC chromatogram (from a methanol/dichloromethane solvent program) of the products of toluene pyrolyzed at 585°C, 110 atm, and 140 sec. Peaks labeled $C_{34}H_{16}$ and $C_{36}H_{16}$ correspond to 10- and 11-ring PAH products, respectively.

Average UV Absorbance (190-520 nm)

Figure 16. HPLC chromatogram of products of Fischer-Tropsch synthetic jet fuel S-8, pyrolyzed at 710 °C and 42 atm, in a scramjet test rig at UTRC. The rise in baseline at ~43 min corresponds to a change in mobile-phase composition to UV-absorbing dichloromethane. Identified components, in order of elution from left to right, are: phenalene, indene, naphthalene, acenaphthylene, 2-methylindene, 1-methylnaphthalene, 2-methylnaphthalene, acenaphthene, phenanthrene, anthracene, cyclopenta[def]phenanthrene, 9-phenylfluorene, 9-methylphenanthrene, fluoranthenene, 1-methylphenanthrene, 1,1'-naphthylanthracene, 1-methylanthracene, pyrene, 2-methylanthracene, 8-methylfluoranthene, 3-methylfluoranthene, benzo[a]fluorene, 4-methylpyrene, 1-phenylpyrene co-eluting with 1-methylpyrene, benzo[a]anthracene, 2,2'-binaphthyl, 2-methylpyrene, chrysene, 2-phenylpyrene, benzo[j]fluoranthene, benzo[a]fluoranthene, benzo[e]pyrene, benzo[k]fluoranthene, perylene, 1-methylchrysene, benzo[k]fluoranthene, benzo[a]pyrene, dibenz[a,h]anthracene, benzo[g,h]perylene, indeno[1,2,3-cd]pyrene, naphtho[2,3-e]pyrene, naphtho[1,1,2-k]fluoranthene, benzo[b]perylene, benzo[b]chrysene coeluting with dibenzo[e,l]pyrene, anthanthrene, picene, dibenzo[b,k]fluoranthene, naphtho[2,3-b]fluoranthene, coronene, naphtho[2,1-a]pyrene, dibenzo[b,g,h]perylene, dibenzo[a,l]pyrene, 1-methylcoronene, phenanthro[2,3-a]pyrene, naphtho[2,3-a]pyrene, dibenzo[b,pq]perylene, benzo[a]anthanthrene, naphtho[8,1,2-bcd]perylene, dibenzo[a,h]pyrene, 2,2'-bianthryl, alkylnaphtho[2,1-a]pyrene, dibenzo[cd,m]perylene, benzo[a]coronene, phenanthro[5,4,3,2-efg,h]perylene, benzo[cd]naphtho[8,1,2,3-fghi]perylene, benzo[g,h]naphtho[8,1,2,3-bcd]perylene, benzo[par]naphtho[8,1,2-bcd]perylene co-eluting with benzo[b]picene, tribenzo[cd,g,h,i,m]perylene, alkyldibenzo[cd,m]perylene, naphtho[8,1,2-abc]coronene, alkylnaphtho[8,1,2-abc]coronene, ovalene, dibenzo[e,g,h]naphtho[8,1,2-kim]perylene and benzo[cd]naphtho[1,2,3-lm]perylene.

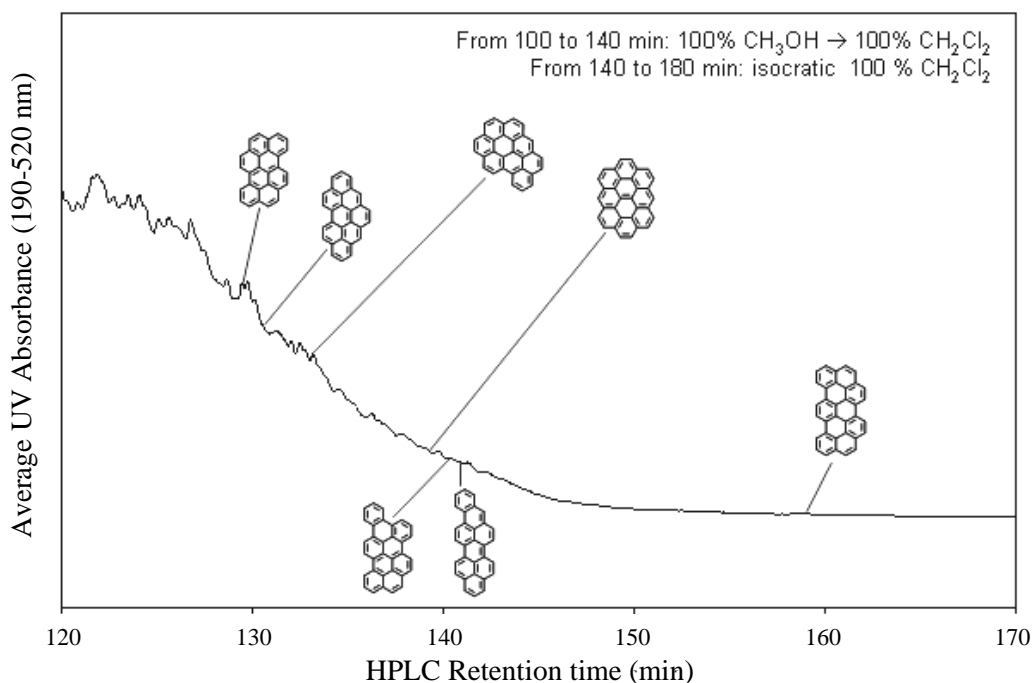


Figure 17. Final portion of the HPLC chromatogram (from a methanol/dichloromethane solvent program) of the products of Fischer-Tropsch synthetic jet fuel S-8, pyrolyzed at 710 °C and 42 atm, in a scramjet test rig at UTRC.

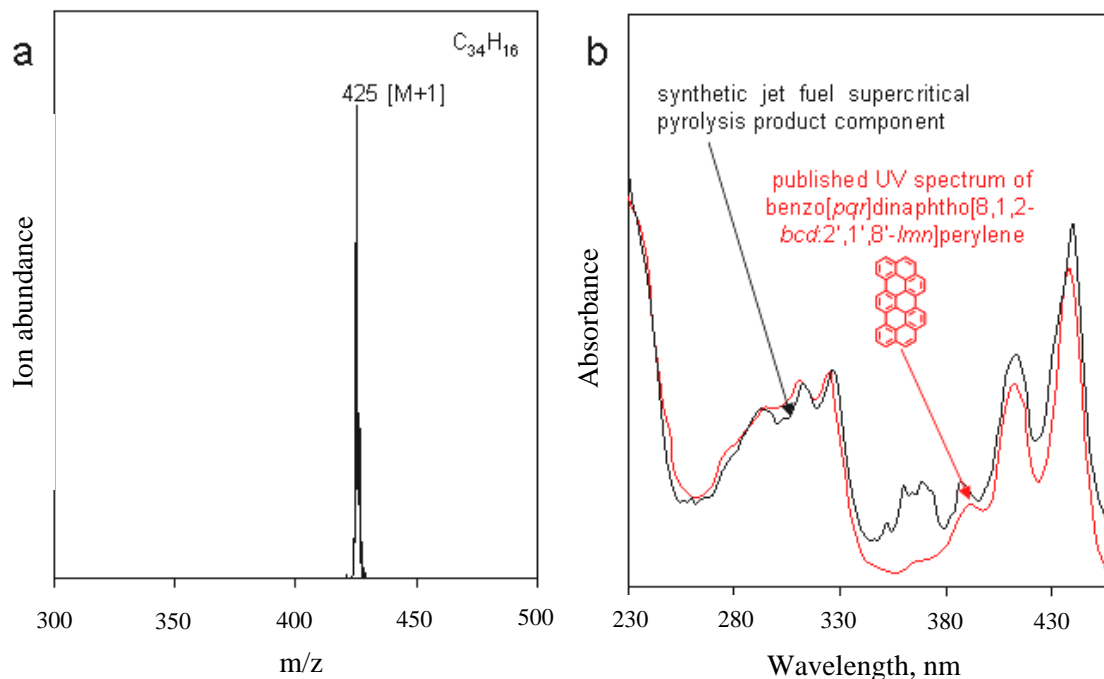


Figure 18. The (a) mass spectrum and (b) UV spectrum of the supercritical Fischer-Tropsch synthetic jet fuel S-8 pyrolysis product component eluting at 159 min in Figure 17. Due to proton transfer from the solvent dichloromethane, the primary ion in the mass spectrum is at $M+1$, so $M = 424$. The published [37] UV spectrum of a reference standard of benzo[*pqr*]dinaphtho[8,1,2-*bcd*:2',1',8'-*lmn*]perylene is included in (b) to confirm the product component's identity as benzo[*pqr*]dinaphtho[8,1,2-*bcd*:2',1',8'-*lmn*]perylene. The spectral signal between 340 and 380 nm is due to an unidentified co-eluting component.